Food Science and Technology 126 (2020): 109315

DOI: https://doi.org/10.1016/j.lwt.2020.109315

Fractionation and precipitation of licorice (*Glycyrrhiza glabra* L.) phytochemicals by supercritical antisolvent (SAS) technique

Somaris E. Quintana*, Diego Martín Hernández, David Villanueva-Bermejo, Mónica R. García-Risco, Tiziana Fornari

Institute of Food Science Research (CIAL), CEI UAM+CSIC, Madrid, Spain

Corresponding author: Somaris E. Quintana. Instituto de Investigación en Ciencias de la Alimentación CIAL (CSIC-UAM), CEI UAM+CSIC, Universidad Autónoma de Madrid, 28049 Madrid, Spain. Phone: +34 910 017 976.

e-mail: somaris.quintana@predoc.uam.es

Abstract

The incorporation of bioactive compounds in food matrices is a priority field of current research in the area of food, nutrition and health. More efficient and environmentally clean technologies, such as supercritical fluid technology, are being studied and developed to achieve this goal. Supercritical anti-solvent precipitation using carbon dioxide constitutes one of these techniques and allows obtaining powdered food ingredients in the form of small size particles, facilitating their incorporation into food matrices and, in addition, increasing the bioavailability of the bioactive compounds. In this work the SAS precipitation of licorice phytochemicals was carried out.

The SAS precipitation of an ethanolic extract of licorice root, obtained by ultrasonic assisted extraction. The products obtained were studied concerning their antioxidant capacity, content of bioactive compounds (liquiritin, liquiritigenin, isoliquiritigenin, glabridin and glycyrrhizic acid), as well as the size and morphology of the particles obtained. SAS technique allows the fractionation of the phytochemicals contained in the ethanolic extract, increasing the antioxidant activity of the precipitates in comparison to that of the original extract. Additionally, it was established the influence of operating conditions to obtain dry, regular and small particles, with an average size of 16 μm under the optimal conditions assessed.

Keywords: Supercritical antisolvent precipitation; Licorice; Antioxidant activity; Morphology; Particle size distribution.

Abbreviations

LES: licorice ethanolic solution

PSD: particle size distribution

SAS: Antisolvent precipitation process

$SCCO_2$: supercritical carbon dioxide

SEM: scanning electron microscopy

TEAC: Trolox equivalent

TPC: Total phenolic compounds

1. Introduction

Licorice (*Glycyrrhiza glabra* L.) grows in Mediterranean countries, Asia and Southeast Europe (Saxena, 2005). Due to its sweet flavor and bioactive properties, licorice was used as a medicinal plant. Recent studies have shown different properties as antitussive, antiulcer, antimicrobial and antiviral, thrombin inhibitor, anti-inflammatory, antidiabetic, hepato-protective and anticancer. These activities were related to the presence of triterpenoid-type and phenolic-type compounds, mainly liquiritin, liquiritigenin, glycyrrhizic acid, isoliquiritigenin and glabridin (Chin et al., 2007; Kaur, Kaur, & Dhindsa, 2013). Extraction techniques like ultrasound assisted extraction (Pan, Liu, Jia, & Shu, 2000), maceration (Sankeshwari, Ankola, Bhat, & Hullatti, 2018), pressurized liquid extraction (Baek, Lee, & Lee, 2008) or supercritical carbon dioxide extraction (Hedayati & Ghoreishi, 2015; S.E. Quintana et al., 2019), were investigated to improve the extraction of licorice bioactive constituents. Natural extracts are in the market in liquid form, as oily preparations, or in solid form as powders. Dried powdered extracts have some advantages over liquid extracts, as higher concentration and stability of the bioactive substances together with lower storage costs (Visentin, Rodríguez-Rojo, Navarrete, Maestri, & Cocero, 2012). Powders containing micro- and/or nano-particles allow a better incorporation of bioactive substances in complex food matrices. Furthermore, smaller sizes improve the bioavailability of bioactive ingredients, increasing absorption and effectiveness (Martín & Cocero, 2008).

Traditionally, size reduction methods were based on physical techniques such as grinding, milling, crystallization or crushing, but these techniques do not allow small enough sizes (Rasenack & Müller, 2004). Nowadays, different techniques have been studied and developed to obtain powdered extracts with small particles, such as spray drying, spray cooling, lyophilization, liquid antisolvent precipitation, among others (X. Chang, Bao, Shan, Bao, & Pan, 2017; Esposito, Roncarati, Cortesi, Cervellati, & Nastruzzi, 2000; Lee et al., 2016; Morita, Horikiri, Suzuki, & Yoshino, 2001). In this respect, the micronization using supercritical fluids has some advantages, such as the possibility of obtaining particles with more homogeneous morphology, narrow particle size distribution (PSD), avoiding the thermal degradation of the product and reducing the use of liquid solvents (Wang, Liu, Wu, & Jiang, 2013). Particularly, supercritical

antisolvent (SAS) precipitation was extensively used in the last years for the production of micro- or nano-particles of pharmaceutical/bioactive compounds (Deshpande et al., 2011; Girotra, Singh, & Nagpal, 2013; Sarkari, Darrat, & Knutson, 2000).

SAS precipitation is based on the continuous contact between supercritical carbon dioxide ($SCCO_2$) and an organic solvent (highly soluble in $SCCO_2$) containing the targeted bioactive compounds. The solution is introduced in the precipitation vessel through a nozzle, forming small drops, together with $SCCO_2$. The $SCCO_2$ penetrate in the droplets, inducing the solution supersaturation, followed by the bioactive substance precipitation (anti-solvent effect) into small solid and dry particles (Langa et al., 2019; Martín & Cocero, 2008).

SAS precipitation conditions should ensure the complete removal of the organic solvent from the precipitation vessel (Reverchon, Torino, Dowy, Braeuer, & Leipertz, 2010). Therefore, the operating conditions depend largely on the solvent used (I. De Marco, Knauer, Cice, Braeuer, & Reverchon, 2012), and specifically on the phase equilibria of the CO_2 + solvent mixture. Thus, to achieve a satisfactory precipitation (small, dry and uniform particles) in SAS method, it is necessary to establish operating conditions above the CO_2 + solvent mixture critical point (MCP) to attain a homogeneous supercritical phase (I. De Marco et al., 2012; Reverchon, Adami, Caputo, & De Marco, 2008; Werling & Debenedetti, 1999). Furthermore, surface tension of the solution (Iolanda De Marco & Reverchon, 2011), fluid dynamics (Badens, Boutin, & Charbit, 2005; Dowy, Braeuer, Schatz, Schluecker, & Leipertz, 2009; Gokhale, Khusid, Dave, & Pfeffer, 2007; Reverchon et al., 2010) and mass transfer (De Diego, Pellikaan, Wubbolts, Witkamp, & Jansens, 2005; Martín & Cocero, 2004, 2008; Mukhopadhyay & Singh, 2004; Werling & Debenedetti, 2000) also influence the morphology and the size of the particles.

Many bioactive pure substances, such as quercetin, caffeine, β-carotene, ellagic acid ibuprofen, mandelic acid, curcumin, among others, were micronized using SAS technique. Specifically, complex mixtures of phytochemicals (e.g. vegetal extracts), such as rosemary (Somaris E. Quintana, Villanueva-Bermejo, Reglero, García-Risco, & Fornari, 2019), mango (Guamán-Balcázar, Montes, Pereyra, & Martínez de la Ossa,

2019), orange (Montes et al., 2019) and yarrow leaves (Villanueva-Bermejo et al., 2017) extracts were simultaneously fractionated and precipitated using SAS. In general, ethanol is the most used organic solvent, due to its high solubility in $SCCO_2$ and extensive use in food applications.

Although the licorice SAS precipitation has not been reported in the literature at present, the extraction of licorice roots has been well studied for the recovery of bioactive phytochemicals. Sohail, Rakha, Butt, & Asghar, (2018) reported a comparison between solid-liquid extraction, using ethanol, methanol and ethyl acetate as solvents, and the $SCCO_2$ extraction of licorice roots. They concluded that the supercritical extracts contained the highest amount of phenolic compounds and flavonoids, and the largest antioxidant capacity. The highest recovery of glycyrrhizic acid and glabridin was obtained at elevated pressures. Quintana et al., (2019) achieved a high antioxidant activity in the extracts obtained using $SCCO_2$ and ethanol as cosolvent. Moreover, two licorice fractions were produced by on-line fractionation with, respectively, antimicrobial and antioxidant activities. Kim et al. [38] studied the effect of different cosolvents on the $SCCO_2$ extraction of glycyrrhizic acid from licorice roots.

In this work, the simultaneous SAS fractionation and precipitation of a licorice ethanolic extract to produce micro- and nano-particles was studied for the first time. The effect of process parameters, e.g. pressure (12.5-20 MPa), temperature (308.15 and 313.15 K) and concentration of licorice phytochemicals in the ethanolic solution (9.6 and 14.2 mg/ml) on the recovery of licorice antioxidants was analyzed, along with the morphology and particle size distribution of the precipitates.

2. Materials and methods

2.1 Chemicals

CO_2 (99.98 % purity) was supplied from Carburos Metálicos (Madrid, Spain). Ethanol (99.8 % purity), Sodium Carbonate anhydrous (99.5% purity) and Folin-Ciocalteu´s reagent were purchased from Panreac (Barcelona, Spain). Gallic acid standard (> 98% purity), 2,2-Diphenyl-1-pycrilhydrazyl (DPPH, 95% purity), (±)-6-Hydroxy-2,5,7,8-tetramethyllchromane-2-carboxylic acid (Trolox, 97% purity), liquiritin, liquiritigenin,

isoliquiritigenin, glabridin and glycyrrhizic acid were purchased from Sigma–Aldrich (St. Louis, MO, USA). Orthophosphoric acid (85% purity) was purchased from Scharlab S.L. (Sentmenat, Spain). Acetonitrile (99,8% purity) was purchased from Macron (Poland).

2.2 Preparation of licorice ethanolic solutions

Roots of licorice harvested in Spain were obtained from Murciana herbalist's (Murcia, Spain) with water content of 9.90% wt. The sample was ground using a Grindomix GM 200 knife mill (Verder International B.V., Vleuten, Netherlands) in particles with size lower than 500 μm. Then, ultrasound assisted extraction (UAE) using an ultrasonic device (Branson Digital Sonifier 550 model, Danbury, USA) with an electric power of 550 W and frequency of 20 kHz was accomplished. The extraction was carried out at 323 K for 15 min using ethanol at 1:10 (w/v) plant/solvent ratio. Extraction yield was 3.18 % (mass of phytochemicals extracted / mass of plant material utilized) and the concentration of licorice phytochemicals in the ethanolic solution was 14.2 mg/ml (LES1). This ethanolic solution (704.2 ml) was further diluted with ethanol to a final volume of 1000 ml to obtain another ethanolic solution containing 9.6 mg/ml (LES2) of licorice phytochemicals. Both ethanolic solutions (14.2 mg/mL and 9.6 mg/mL) were stored at 253.15 K for its use in the SAS process.

2.3 Supercritical antisolvent (SAS) precipitation

Figure 1 shows the supercritical antisolvent precipitation device used for this study (Model Thar SF2000, Thar Technology, PA, USA). A detailed description of the equipment can be found elsewhere [36]. The equipment comprises a precipitation vessel and a separator with independent control of temperature and pressure. The precipitation vessel (273 ml) is equipped with a 101.6 μm inner diameter nozzle to spray the ethanolic solution. $SCCO_2$ and the ethanolic solution are fed from the top in a co-current manner (coaxial nozzle).

$SCCO_2$ was pumped at 50 g/min flow rate until pressure and temperature conditions were attained into the precipitation vessel. Then, the licorice ethanolic solution (LES) was pumped through the nozzle at 2 g/min for 45 min, while maintaining the $SCCO_2$

flow rate. Additional $SCCO_2$ was pumped during 15 min to wash out the residual solvent from the precipitator. During the process, the separator was kept at 313.15 K and ambient pressure. In the separator, ethanol and the phytochemicals which did not precipitate into the precipitation vessel (i.e. the licorice phytochemicals which are soluble in the $SCCO_2$+ethanol supercritical phase) were recovered. Finally, the precipitation vessel was depressurized, and the precipitate was collected from a frit placed at the bottom of the precipitator vessel. The ethanolic fraction was further rotary evaporated until an oleoresin-type product was obtained. Samples (oleoresins and precipitates) were kept at 253.15 K under darkness until analysis.

2.4 Total phenolic compounds and antioxidant activity

Folin-Ciocalteu method (Singleton, Orthofer, & Lamuela-Raventós, 1999) was used to determine the total phenolic compounds (TPC) content in the samples. Sample (50 µL) was mixed with 3 ml of milliQ water and 250 µl of the Folin Ciocalteu reagent and strongly mixed. After 3 min, 750 µl of sodium carbonate solution (20% mass) and 950 µl of milliQ water were added. After 2 h at room temperature in darkness, the absorbance was measured at 760 nm using a Genesys 10S UV-Vis spectrophotometer (Thermo Fischer Scientific Inc., MA, USA). A calibration curve (linear regression) was utilized to calculate the TPC concentration in the samples and TPC values were expressed as GAE (mg of gallic acid equivalents / g of sample).

The method described by Brand-Williams, Cuvelier, & Berset, (1995) was used to determine the antioxidant capacity of the samples. Sample (25 µL) was added to 975 µl of the DPPH radical in ethanol (23.5 µg/ml). The radical scavenging reaction was carried out at room temperature and under darkness for 2 h. Then, the absorbance was measured at 515 nm in a Genesys 10S UV-Vis spectrophotometer (Thermo Fischer scientific, MA, USA). A calibration curve (linear regression) was utilized to calculate the DPPH concentration in the reaction medium. Pure solvent was used as control, to measure the maximum DPPH absorbance. Trolox was used as reference standard and the results were expressed as TEAC values (mmol Trolox equivalent/g extract). All analyses were done in triplicate.

2.5 HPLC-DAD analysis

HPLC analysis was carried out as described by Wei, Yang, Chen, Wang, & Cui, (2015). A LC-2030C 3D Plus (Shimadzu) device equipped with a quaternary pump, auto-injector and DAD detector was used. The column was ACE Kromasil 100 C18 (250 x 4.6 mm; 5 μm) and analyses were accomplished at 298 K. The mobile phase comprised acetonitrile (A) and 0.026% aqueous H_3PO_4 (v/v), and the following elution gradient was applied: 20-25% A for 0-20 min, 25-34% A for 20-30 min, 34-50% A for 30-50 min, 50-60% A at 50-60 min and 60% A for 60-80 min. The initial conditions were attained in 5 min. The flow rate was 0.7 ml/min and was kept constant throughout the analysis. The injection volume was 20 μl and the detections were carried out at 230, 254, 280 and 370 nm. Calibration curves with standards were used to determine the content of the bioactive licorice phytochemicals (liquiritin, liquiritigenin, isoliquiritigenin, glabridin and glycyrrhizic acid) in the different samples.

2.6 Morphology and Particle size analysis

The morphology of precipitates was studied by scanning electron microscopy (SEM) with an energy-dispersive X-ray spectrometer (SEM-EDS) XL-30S FEG, Philips (Japan). Samples were placed on carbon tapes and then were coated with a thin chrome layer by a sputter coater. Particle size and size distributions were measured by light scattering with a laser diffraction system Mastersizer 2000 (Malvern Instruments Ltd., Malvern, UK), equipped with a wet dispersion unit.

3. Results and Discussion

3.1 The supercritical antisolvent process

The CO_2 + ethanol + licorice phytochemicals is a complex multicomponent system and the phase equilibria of this mixture strongly affect the performance and the result of SAS process. Particularly, the temperature and pressure of the mixture critical point (MCP) in comparison with SAS temperature and pressure conditions may determine the success of the precipitation process, since affect jet mixing, fluid dynamics and mass transfer (Reverchon et al., 2010). These complex mechanisms are responsible for the great variety of particle sizes and morphologies that can be obtained in SAS precipitation process. Particularly, as mentioned before, it was described in the literature

(Reverchon et al., 2010) that these mechanisms strongly depend on the SAS temperature and pressure conditions, which can be located below the MCP, near above the MCP or far above the MCP Figure 2).

In general, it was stated (Reverchon & De Marco, 2011) that when SAS conditions are below the MCP but in the homogenous subcritical region, the formation of particles is induced by the $SCCO_2$ antisolvent effect and by the organic solvent depletion in the droplets formed by the nozzle. Consequently, microparticles and expanded microparticles (hollow core particles) with irregular forms are obtained. Nevertheless, if the SAS subcritical conditions are located within the liquid-vapor region, irregular particles and agglomerates are produced due to the presence of residual solvent in the precipitate. On the other hand, when SAS conditions are far above the MCP, the mixing of CO_2 with the solvent is produced instantaneously and no liquid-gas interphase occurs, resulting in smaller and more regular particles due to their condensation from a gaseous phase.

Due to the lack of information about phase equilibria of the complex mixtures CO_2 + ethanol + licorice phytochemicals, the $SCCO_2$ and licorice ethanolic solution (LES) flow rates were established with the aim of attaining a homogenous supercritical phase (≈ 3 % mass ethanol) at the pressures and temperatures studied, according to the CO_2 + ethanol binary phase equilibria data (C. J. Chang, Day, Ko, & Chiu, 1997; Joung et al., 2001; Knez, Škerget, Ilič, & Lütge, 2008; Reverchon & De Marco, 2011). Indeed, this is an approximation, since the presence of a large number and varied phytochemicals in the supercritical phase may really change the MPC in comparison with that of the binary CO_2 + ethanol.

3.2. Effect of the concentration of phytochemicals in the licorice ethanolic solution

Table 1 shows the results obtained by SAS with LES1 (14.2 mg/ml) at different precipitation pressures and temperatures. The table reports the precipitate and oleoresin yields, TPC, TEAC and IC_{50} values, obtained from the different samples collected. All SAS experiments were carried out by duplicate and the average deviations are given (Table 1).

A significant decrease in the precipitation yields was observed at 313.15 K (experiments 1 and 2 in Table 1) in comparison with the rest of experiments. These precipitates were very viscous, with large agglomerates adhered to the precipitation vessel walls, and they were difficult to recover and to quantify their weight and thus, high deviations were obtained. On the other hand, for the rest of experiments reported in Table 1, which were performed at 308.15 K, solid and dry powders were obtained, and the average deviation of precipitation yields between duplicates was always less than 9.21 % (mean deviation of 3.96 %).

Table 2 show SAS precipitation assays when the concentration of the licorice ethanolic solution was 9.6 mg/ml (LES2). Experiments were carried out at 308.15 and 313.15 K and pressures of 15 and 20 MPa. No duplicates were accomplished and thus, no average deviations are given for process yields. Yet, the TPC, antioxidant activity (TEAC and IC_{50} values) determinations were carried out by triplicate and the average deviations of these data are included in Table 2.

In all the experiments reported in Table 2, homogeneous particles were obtained in dry powders, including those assays carried out at 313.15 K. The different behavior observed at this temperature when using the different licorice ethanolic solutions, may be due to an expected higher MCP of LES1 in comparison with the MCP of LES2, as a result of the higher concentration of phytochemicals in LES1. Thus, it is possible that SAS operation conditions were subcritical for LES1 while supercritical for LES2. Furthermore, higher concentration of phytochemicals results in higher solution viscosity and may impair atomization, as reported by Prosapio, De Marco, & Reverchon, (2018). Then, experiments with LES1 at 313.15 K lead to the coalescence of particles, forming agglomerates, while experiments with LES2 at the same temperature resulted in dry powders.

Additionally, it can be observed from Tables 1 and 2 that precipitate, and oleoresin yields were higher using LES2 than using LES1. Thus, the total yields of SAS process (precipitate + oleoresin) were higher at the lower concentration of the licorice ethanolic solution used. For example, experiment 7 in Table 2 shows a 1.5-fold increase of

process yield (91 %) in comparison with its counterpart at 14.2 mg/ml (experiment 4 in Table 1).

3.2. Effect of pressure and temperature in SAS process yields

Figure 3 shows that at constant temperature (308.15 K) and constant licorice ethanolic concentration (LES1) the lower pressures brought about higher precipitate yields than oleoresin yields, while the opposite effect occurred at the higher pressures. As the pressure in the precipitation vessel increases at constant temperature, the $SCCO_2$ density increases and thus, the solubility of licorice phytochemicals in the supercritical phase also increases, resulting in a decrease of precipitation yield. Then, while lower amounts of solid powders are recovered in the precipitates, larger amounts of oleoresins are recovered from the separator. Furthermore, it can be observed that total recovery (mass of precipitate + oleoresin) of licorice phytochemicals feed into the SAS process reached values in the range 58-67% (experiments 3-6 in Table 1).

The general tendency observed with LES1 concerning the effect of pressure was also observed with LES2 (i.e. exp. 7 and 8 at 308.15 K, and exp. 9 and 10 at 313.15 K) but the total recovery of licorice phytochemicals in this case was higher and in the range of 68-91% (Table 2).

Regarding the effect of temperature, it can be observed that at lower pressures a decrease in temperature favors the precipitate yields, as indicated by the results of Table 1 (exp. 1 and 4) and Table 2 (exp. 7 and 9), all them carried out at 15 MPa. Consequently, the increase in temperature produced an increase in the oleoresin yields. However, at the higher pressures (20 MPa) the effect of temperature seems to be less important.

3.2 Phenolic compounds and antioxidant activity of precipitates and oleoresins

Figure 4 shows the recovery of total phenolic compounds obtained in the precipitation vessel as a function of pressure and concentration of licorice phytochemicals in the ethanolic solution. The TPC recoveries were higher with the lower concentration of the licorice ethanolic solution. Furthermore, a tendency to obtain higher TPC recoveries at

302 the lower pressures can also be observed. Within the range of SAS operation conditions
303 studied, the best conditions to recover in the precipitate the licorice phenolic compounds
304 would be 15 MPa, 308.15 K and 9.6 mg/ml licorice ethanolic solution. At these
305 conditions high concentration (160.8 mg GAE/g) and yield (≈ 71 %) of TPC was
306 obtained, and also adequate precipitation yield (52.7%) was achieved. Taking into
307 account that the original licorice root ultrasound extract contains 119.5 ± 4.1 mg
308 GAE/g, an increase in the concentration of TPC was observed in the precipitates, with
309 values up to 1.4 greater.

310 Since phenolic compounds are substances with recognized antioxidant activity it is
311 generally stated that the higher the TPC the higher the antioxidant activity, that is the
312 higher TEAC values and the lower IC_{50} values. The TEAC and IC_{50} values obtained in
313 precipitates and oleoresins are depicted in Figure 5 as a function of TPC. In general, as
314 can be observed in Figure 5(a), there is no clear relationship (e.g. linear relation)
315 between TEAC and TPC values but is apparent that the precipitates presented higher
316 TEAC values than oleoresins for the same TPC concentration. This means that different
317 type and phenolic compound composition are present in precipitates and oleoresins,
318 being the TPC in the precipitate of greater antioxidant capacity. Accordingly, the IC_{50}
319 values of the precipitates are lower than those corresponding to oleoresins, as can be
320 seen in Figure 5(b).

321 **3.3 SAS fractionation of licorice phytochemicals**

322 As mentioned before, in the case of SAS precipitation of ethanolic plant extracts, the
323 fractionation of its bioactive substances is generally carried out, due to the different
324 solubility of the plant extract components in the supercritical CO_2 + ethanol phase
325 (Villanueva-Bermejo et al., 2017; Villanueva Bermejo et al., 2015).

326 Table 3 presents some key licorice bioactive compounds (Figure 6) identified in both,
327 precipitates and oleoresins. In general, liquiritigenin, glabridin and isoliquiritigenin
328 compounds are more abundant in the oleoresins, while liquiritin and glycyrrhizic acid
329 are concentrated in the precipitates. The observed trend may be explained considering
330 the polarity of these compounds, which is related to their chemical structure.

The most polar compounds are less soluble in the supercritical phase (CO_2 + ethanol cosolvent) and thus these polar compounds should preferable precipitate. On the contrary, the less polar compounds (more soluble in the supercritical phase) should be preferable recovered in the separator, together with the ethanol cosolvent. Both liquiritigenin and glabridin are the most non-polar compounds identified, with only two hydroxyl groups in their structure. Isoliquiritigenin has a structure similar to liquiritigenin but the latter is a flavanone and isoliquiritigenin is a chalcone (flavanone precursor). The chalcones have the central ring open, so they have a free hydroxyl group that gives it greater polarity compared to the flavone liquiritigenin. Glycyrrhizic acid is a glycosylated terpenoid, and despite its terpenoid part, the glycosylated sugar provides some polarity to this acid, producing its concentration in the precipitate. Finally, liquiritin is the most polar compound of those studied (with 5 hydroxyl groups in its chemical structure) and it is observed that it is most abundant in the precipitate.

Figure 7 shows for experiments 3 to 6 (308.15 K and 14.2 mg/ml of the licorice ethanolic solution) the variation with pressure of the precipitate IC_{50} values and the sum of the concentrations (mg/g) of the compounds identified and quantified by HPLC (Table 3). The IC_{50} values decrease with decreasing pressure while the content of these compounds in the precipitates increases. That is, the precipitates present better antioxidant activity and contain large amounts of licorice key bioactives at the lower precipitation pressures. This trend was verified for the sum of the concentrations of all identified compounds, as well as for the concentration of liquiritin and glabridin, which are the most abundant compounds within those identified. Therefore, it could be concluded that key licorice root compounds of Table 3 have a significant effect on the antioxidant activity of the precipitates. This conclusion is in accordance with Kaur et al., (2013), who pointed out glabridin and isoliquiritigenin as key compounds responsible for the antioxidant activity of licorice root.

3.4 Morphology and particle size of precipitates

Taking into account the phase equilibria of the binary CO_2 + ethanol mixture [43-45] the corresponding critical pressures at 308.15 K and 313.15 K are both lower than 10 MPa. Thus, considering the binary mixture, the operating conditions set for all the

experiments in Tables 1 and 2 should be above the MCP (supercritical homogeneous phase region of Figure 2) and no liquid-gas interphase should occur, which could lead to the formation of small and uniform particles. Nevertheless, as stated before, in the case of the precipitation of vegetal extracts, the presence of a large variety of phytochemicals in the organic solution may change significantly the MCP of the supercritical phase. Figure 8 shows the morphology (SEM imagens) resulted in experiments 1 and 2 of Table 1. As can be clearly deduced from the figure, the morphology obtained in experiments 1 and 2 are very different from those resulted in the rest of experiments. A semi-continuous material is observed, more similar to a gum-resin, with cavities within the aggregates. These images might corroborate that SAS operating conditions in these experiments were below the MCP, probably in the two-phase region of Figure 2, as a result of the higher temperature and higher concentration of phytochemicals in the ethanolic solution. Figure 9 show SEM imagens at a lower scale (75x) of the precipitates obtained in experiments 1 and 2, where it can be observed adjoined particles (coalescence phenomenon) in large sizes, especially at 15 MPa (experiment 1).

On the other hand, for the rest of experiments of Figure 8, particles with similar morphology and micronized size were obtained. Nevertheless, uniform and spherical structures in the precipitates were not obtained probably due to precipitation conditions in the subcritical region (see Figure 2) since, as mentioned before, uniform and small spherical particles (nanoparticles) are generally obtained at pressures larger than those corresponding to the MCP (Reverchon et al., 2008, 2010; Werling & Debenedetti, 2000).

The mean particle size and size distribution of the precipitates are given in Table 4. Furthermore, for experiments 3 to 6 the particle size distributions of duplicate experiments are depicted in Figure 10. Deviations are in the range 1.1-3.4 μm (< 10%). It can be observed that at constant temperature (308.15 K) and concentration of the licorice ethanolic solution (14.2 mg/g) the mean particle size of the precipitated powders decreases with pressure, from 36.7 μm at 12.5 MPa to 11.7 μm at 25 MPa. In addition, it could be inferred from Figure 10 that at the higher pressures the particle sizes are somewhat more heterogeneous. The distribution at the lower pressure (12.5

391 MPa) is narrower and more normal, while increasing pressure the behavior appears as a
392 multi-modal distribution, with significant smaller sizes.

393 This tendency of particle size decrease with an increase in the precipitation pressure is
394 consistent with the analysis published by Werling & Debenedetti, (1999) and Martín &
395 Cocero, (2004) in their SAS precipitation simulation models. Furthermore, several
396 experimental works confirm this tendency, such as the SAS precipitation of tartaric acid
397 reported by Kröber & Teipel, (2002), the *Achilea millefolium* L. ethanolic extract
398 studied by Villanueva-Bermejo et al., (2017), and mango leaf extracts carried out by
399 Guamán-Balcázar et al., (2019).

400 Besides the effect of pressure on particle size, it can be observed in the SEM imagens
401 presented in Figure 11 that decreasing the concentration of the licorice ethanolic
402 solution smaller particles are obtained. The lower the concentration of licorice
403 phytochemicals in the ethanolic solution, the more similar MCP of the supercritical
404 phase to that of the binary CO_2 + ethanol, and thus the precipitation conditions
405 established are closer to be in the supercritical homogenous region.

406 **4. Conclusions**

407 Selecting adequate operating conditions, the supercritical anti-solvent SAS precipitation
408 of licorice ethanolic solutions produced the fractionation of licorice phytochemicals: dry
409 powders with small aggregate particles together with oleoresin by-product were
410 obtained. The higher precipitation yields were obtained at the lower pressures and
411 temperatures, and yield increases as the concentration of licorice phytochemicals in the
412 ethanolic solution decreases from 14.2 to 9.6 mg/ml, being the highest yield (52.70%)
413 obtained at 15MPa, 308.15 K and 9.6 mg/ml.

414 In general, it was observed an increase of the recovery of phenolic phytochemicals in
415 the precipitates as the pressure, temperature and concentration of the licorice ethanolic
416 solution decreases. Within the operating range studied, the optimum corresponds to 15
417 MPa, 308.15 K and 9.6 mg/ml, with a 1.3 enrichment factor with respect to the licorice
418 extract. Furthermore, the precipitates have better antioxidant activity than the oleoresins
419 for the same concentration of total phenolic compounds, due to the fractionation caused

by SAS technique resulting in different type of phenolic compounds in precipitates and oleoresins. Liquiritin and glabridin are abundant in the precipitates, and the IC_{50} values decrease (better antioxidant activity) as their concentration in the precipitates increases.

Particles with smaller size were obtained with increasing pressure and decreasing the concentration of phytochemicals in the licorice ethanolic solution. Nevertheless, agglomerated particles were obtained, probably due to precipitation conditions in the range below the supercritical multicomponent (phytochemicals + CO_2 + ethanol) mixture critical point. It is highlighted the importance of SAS operating conditions well above the critical point of the supercritical mixture to obtain an adequate morphology with regular and spherical particles.

Acknowledgement

The authors gratefully acknowledge the financial support from Ministerio de Economía y Competitividad of Spain (Projects AGL2017-89055-R and AGL2016-76736-C3-1-R). Somaris E. Quintana is grateful for the funding provided by Gobernación de Bolivar and Fundación Ceiba, Colombia, in the project "Bolívar Gana con Ciencia".

References

Badens, E., Boutin, O., & Charbit, G. (2005). Laminar jet dispersion and jet atomization in pressurized carbon dioxide. *The Journal of Supercritical Fluids*, *36*(1), 81–90. https://doi.org/10.1016/J.SUPFLU.2005.03.007

Baek, J. Y., Lee, J. M., & Lee, S. C. (2008). Extraction of nutraceutical compounds from licorice roots with subcritical water. *Separation and Purification Technology*, *63*(3), 661–664. https://doi.org/10.1016/j.seppur.2008.07.005

Brand-Williams, W., Cuvelier, M. E., & Berset, C. (1995). Use of a Free Radical Method to Evaluate Antioxidant Activity, *28*, 25–30.

Chang, C. J., Day, C. Y., Ko, C. M., & Chiu, K. L. (1997). Densities and P-x-y diagrams for carbon dioxide dissolution in methanol, ethanol, and acetone mixtures. *Fluid Phase Equilibria*, *131*(1–2), 243–258. https://doi.org/10.1016/s0378-3812(96)03208-6

Chang, X., Bao, J., Shan, G., Bao, Y., & Pan, P. (2017). Crystallization-Driven Formation of Diversified Assemblies for Supramolecular Poly(lactic acid)s in Solution. *Crystal Growth & Design*, *17*(5), 2498–2506. https://doi.org/10.1021/acs.cgd.7b00013

Chin, Y.-W., Jung, H.-A., Liu, Y., Su, B.-N., Castoro, J. A., Keller, W. J., Kinghorn, A. D. (2007). Anti-oxidant Constituents of the Roots and Stolons of Licorice (*Glycyrrhiza glabra*). https://doi.org/10.1021/jf0703553

De Diego, Y. P., Pellikaan, H. C., Wubbolts, F. E., Witkamp, G. J., & Jansens, P. J. (2005). Operating regimes and mechanism of particle formation during the precipitation of polymers using the PCA process. *Journal of Supercritical Fluids*, *35*(2), 147–156. https://doi.org/10.1016/j.supflu.2004.12.012

De Marco, I., Knauer, O., Cice, F., Braeuer, A., & Reverchon, E. (2012). Interactions of phase equilibria, jet fluid dynamics and mass transfer during supercritical antisolvent micronization: The influence of solvents. *Chemical Engineering Journal*, *203*, 71–80. https://doi.org/10.1016/J.CEJ.2012.06.129

De Marco, Iolanda, & Reverchon, E. (2011). Influence of pressure, temperature and concentration on the mechanisms of particle precipitation in supercritical

antisolvent micronization. *Journal of Supercritical Fluids*, *58*(2), 295–302. https://doi.org/10.1016/j.supflu.2011.06.005

Deshpande, P. B., Kumar, G. A., Kumar, A. R., Shavi, G. V., Karthik, A., Reddy, M. S., & Udupa, N. (2011). Supercritical Fluid Technology: Concepts and Pharmaceutical Applications. *PDA Journal of Pharmaceutical Science and Technology*, *65*(3), 333–344. https://doi.org/10.5731/pdajpst.2011.00717

Dowy, S., Braeuer, A., Schatz, R., Schluecker, E., & Leipertz, A. (2009). CO_2 partial density distribution during high-pressure mixing with ethanol in the supercritical antisolvent process. *Journal of Supercritical Fluids*, *48*(3), 195–202. https://doi.org/10.1016/j.supflu.2008.10.017

Esposito, E., Roncarati, R., Cortesi, R., Cervellati, F., & Nastruzzi, C. (2000). Production of Eudragit microparticles by spray-drying technique: Influence of experimental parameters on morphological and dimensional characteristics. *Pharmaceutical Development and Technology*, *5*(2), 267–278. https://doi.org/10.1081/PDT-100100541

Girotra, P., Singh, S. K., & Nagpal, K. (2013). Supercritical fluid technology: a promising approach in pharmaceutical research. *Pharmaceutical Development and Technology*, *18*(1), 22–38. https://doi.org/10.3109/10837450.2012.726998

Gokhale, A., Khusid, B., Dave, R. N., & Pfeffer, R. (2007). Effect of solvent strength and operating pressure on the formation of submicrometer polymer particles in supercritical microjets. *Journal of Supercritical Fluids*, *43*(2), 341–356. https://doi.org/10.1016/j.supflu.2007.05.012

Guamán-Balcázar, M. C., Montes, A., Pereyra, C., & Martínez de la Ossa, E. (2019). Production of submicron particles of the antioxidants of mango leaves/PVP by supercritical antisolvent extraction process. *Journal of Supercritical Fluids*, *143*(July 2018), 294–304. https://doi.org/10.1016/j.supflu.2018.09.007

Hedayati, A., & Ghoreishi, S. M. (2015). Supercritical carbon dioxide extraction of glycyrrhizic acid from licorice plant root using binary entrainer: Experimental optimization via response surface methodology. *Journal of Supercritical Fluids*, *100*, 209–217. https://doi.org/10.1016/j.supflu.2015.03.005

Joung, S. N., Yoo, C. W., Shin, H. Y., Kim, S. Y., Yoo, K. P., Lee, C. S., & Huh, W. S. (2001). Measurements and correlation of high-pressure VLE of binary CO_2 - alcohol systems (methanol, ethanol, 2-methoxyethanol and 2-ethoxyethanol). *Fluid Phase Equilibria*, *185*(1–2), 219–230. https://doi.org/10.1016/S0378-3812(01)00472-1

Kaur, R., Kaur, H., & Dhindsa, A. S. (2013). Glycyrrhiza glabra: a phytopharmacological review. *International Journal of Pharmaceutical Sciences and Research*, *4*(7), 2470–2477. https://doi.org/10.13040/IJPSR.0975-8232.4(7).2470-77

Knez, Ž., Škerget, M., Ilič, L., & Lütge, C. (2008). Vapor-liquid equilibrium of binary CO_2-organic solvent systems (ethanol, tetrahydrofuran, ortho-xylene, meta-xylene, para-xylene). *Journal of Supercritical Fluids*, *43*(3), 383–389. https://doi.org/10.1016/j.supflu.2007.07.020

Kröber, H., & Teipel, U. (2002). Materials processing with supercritical antisolvent precipitation: Process parameters and morphology of tartaric acid. *Journal of Supercritical Fluids*, *22*(3), 229–235. https://doi.org/10.1016/S0896-8446(01)00124-3

Langa, E., Pardo, J. I., Giménez-Rota, C., González-Coloma, A., Hernáiz, M. J., & Mainar, A. M. (2019). Supercritical anti-solvent fractionation of Artemisia absinthium L. conventional extracts: tracking artemetin and casticin. *Journal of Supercritical Fluids*, *151*, 15–23. https://doi.org/10.1016/j.supflu.2019.05.003

Lee, H. J., Kang, J. H., Lee, H. G., Kim, D. W., Rhee, Y. S., Kim, J. Y., … Park, C. W. (2016). Preparation and physicochemical characterization of spray-dried and jet-milled microparticles containing bosentan hydrate for dry powder inhalation aerosols. *Drug Design, Development and Therapy*, *10*, 4017–4030. https://doi.org/10.2147/DDDT.S120356

Martín, A., & Cocero, M. J. (2004). Numerical modeling of jet hydrodynamics, mass transfer, and crystallization kinetics in the supercritical antisolvent (SAS) process. *Journal of Supercritical Fluids*, *32*(1–3), 203–219. https://doi.org/10.1016/j.supflu.2004.02.009

Martín, A., & Cocero, M. J. (2008). Micronization processes with supercritical fluids:

526 Fundamentals and mechanisms. *Advanced Drug Delivery Reviews*, *60*(3), 339–
527 350. https://doi.org/10.1016/J.ADDR.2007.06.019

528 Montes, A., Hanke, F., Williamson, D., Guamán-Balcázar, M. C., Valor, D., Pereyra,
529 C., Martínez De La Ossa, E. (2019). Precipitation of powerful antioxidant
530 nanoparticles from orange leaves by means of supercritical CO2. *Journal of CO2*
531 *Utilization*, *31*, 235–243. https://doi.org/10.1016/j.jcou.2019.03.021

532 Morita, T., Horikiri, Y., Suzuki, T., & Yoshino, H. (2001). Preparation of gelatin
533 microparticles by co-lyophilization with poly(ethylene glycol): Characterization
534 and application to entrapment into biodegradable microspheres. *International*
535 *Journal of Pharmaceutics*, *219*(1–2), 127–137. https://doi.org/10.1016/S0378-
536 5173(01)00642-1

537 Mukhopadhyay, M., & Singh, S. (2004). Refining of crude lecithin using dense carbon
538 dioxide as anti-solvent. *Journal of Supercritical Fluids*, *30*(2), 201–211.
539 https://doi.org/10.1016/j.supflu.2003.08.001

540 Pan, X., Liu, H., Jia, G., & Shu, Y. Y. (2000). Microwave-assisted extraction of
541 glycyrrhizic acid from licorice root. *Biochemical Engineering Journal*, *5*(3), 173–
542 177. https://doi.org/10.1016/S1369-703X(00)00057-7

543 Prosapio, V., De Marco, I., & Reverchon, E. (2018). Supercritical antisolvent
544 coprecipitation mechanisms. *The Journal of Supercritical Fluids*, *138*, 247–258.
545 https://doi.org/10.1016/J.SUPFLU.2018.04.021

546 Quintana, S.E., Cueva, C., Villanueva-Bermejo, D., Moreno-Arribas, M. V., Fornari, T.,
547 & García-Risco, M. R. (2019). Antioxidant and antimicrobial assessment of
548 licorice supercritical extracts. *Industrial Crops and Products*, *139*.
549 https://doi.org/10.1016/j.indcrop.2019.111496

550 Quintana, Somaris E., Villanueva-Bermejo, D., Reglero, G., García-Risco, M. R., &
551 Fornari, T. (2019). Supercritical antisolvent particle precipitation and fractionation
552 of rosemary (*Rosmarinus officinalis* L.) extracts. *Journal of CO2 Utilization*, *34*,
553 479–489. https://doi.org/10.1016/j.jcou.2019.07.032

554 Rasenack, N., & Müller, B. W. (2004). Micron-Size Drug Particles: Common and
555 Novel Micronization Techniques. *Pharmaceutical Development and Technology*.

556 https://doi.org/10.1081/PDT-120027417

557 Reverchon, E., Adami, R., Caputo, G., & De Marco, I. (2008). Spherical microparticles
558 production by supercritical antisolvent precipitation: Interpretation of results. *The*
559 *Journal of Supercritical Fluids*, *47*(1), 70–84.
560 https://doi.org/10.1016/J.SUPFLU.2008.06.002

561 Reverchon, E., & De Marco, I. (2011). Mechanisms controlling supercritical antisolvent
562 precipitate morphology. *Chemical Engineering Journal*, *169*(1–3), 358–370.
563 https://doi.org/10.1016/J.CEJ.2011.02.064

564 Reverchon, E., Torino, E., Dowy, S., Braeuer, A., & Leipertz, A. (2010). Interactions of
565 phase equilibria, jet fluid dynamics and mass transfer during supercritical
566 antisolvent micronization. *Chemical Engineering Journal*, *156*(2), 446–458.
567 https://doi.org/10.1016/j.cej.2009.10.052

568 Sankeshwari, R., Ankola, A., Bhat, K., & Hullatti, K. (2018). Soxhlet versus cold
569 maceration: Which method gives better antimicrobial activity to licorice extract
570 against Streptococcus mutans? *Journal of the Scientific Society*, *45*(2), 67.
571 https://doi.org/10.4103/jss.jss_27_18

572 Sarkari, M., Darrat, I., & Knutson, B. L. (2000). Generation of microparticles using
573 CO2 and CO2-philic antisolvents. *AIChE Journal*, *46*(9), 1850–1859.
574 https://doi.org/10.1002/aic.690460913

575 Saxena, S. (2005). Natural Product Radiance Glycyrrhiza glabra: Medicine over the
576 millennium. *Natural Product Radiance*, *4*(5), 358–367.

577 Singleton, V. L., Orthofer, R., & Lamuela-Raventós, R. M. (1999). [14] Analysis of
578 total phenols and other oxidation substrates and antioxidants by means of folin-
579 ciocalteu reagent. *Methods in Enzymology*, *299*, 152–178.
580 https://doi.org/10.1016/S0076-6879(99)99017-1

581 Sohail, M., Rakha, A., Butt, M. S., & Asghar, M. (2018). Investigating the antioxidant
582 potential of licorice extracts obtained through different extraction modes. *Journal*
583 *of Food Biochemistry*, *42*(2), e12466. https://doi.org/10.1111/jfbc.12466

584 Villanueva-Bermejo, D., Zahran, F., Troconis, D., Villalva, M., Reglero, G., & Fornari,
585 T. (2017). Selective precipitation of phenolic compounds from *Achillea*

586 *millefolium* L. extracts by supercritical anti-solvent technique. *Journal of*
587 *Supercritical Fluids*, *120*, 52–58. https://doi.org/10.1016/j.supflu.2016.10.011

588 Villanueva Bermejo, D., Ibáñez, E., Reglero, G., Turner, C., Fornari, T., & Rodriguez-
589 Meizoso, I. (2015). High catechins/low caffeine powder from green tea leaves by
590 pressurized liquid extraction and supercritical antisolvent precipitation. *Separation*
591 *and Purification Technology*, *148*, 49–56.
592 https://doi.org/10.1016/j.seppur.2015.04.037

593 Visentin, A., Rodríguez-Rojo, S., Navarrete, A., Maestri, D., & Cocero, M. J. (2012).
594 Precipitation and encapsulation of rosemary antioxidants by supercritical
595 antisolvent process. *Journal of Food Engineering*, *109*, 9–15.
596 https://doi.org/10.1016/j.jfoodeng.2011.10.015

597 Wang, W., Liu, G., Wu, J., & Jiang, Y. (2013). Co-precipitation of 10-
598 hydroxycamptothecin and poly (l-lactic acid) by supercritical CO2 anti-solvent
599 process using dichloromethane/ethanol co-solvent. *Journal of Supercritical Fluids*,
600 *74*, 137–144. https://doi.org/10.1016/j.supflu.2012.11.022

601 Wei, S.-S., Yang, M., Chen, X., Wang, Q.-R., & Cui, Y.-J. (2015). Simultaneous
602 determination and assignment of 13 major flavonoids and glycyrrhizic acid in
603 licorices by HPLC-DAD and Orbirap mass spectrometry analyses. *Chinese*
604 *Journal of Natural Medicines*, *13*(3), 232–240. https://doi.org/10.1016/S1875-
605 5364(15)30009-1

606 Werling, J. O., & Debenedetti, P. G. (1999). Numerical modeling of mass transfer in the
607 supercritical antisolvent process. *The Journal of Supercritical Fluids*, *16*(2), 167–
608 181. https://doi.org/10.1016/S0896-8446(99)00027-3

609 Werling, J. O., & Debenedetti, P. G. (2000). Numerical modeling of mass transfer in the
610 supercritical antisolvent process: Miscible conditions. *Journal of Supercritical*
611 *Fluids*, *18*(1), 11–24. https://doi.org/10.1016/S0896-8446(00)00054-1

612

Table 1. SAS conditions in the fractionation and precipitation of licorice ethanolic solution (LES). Yield (Y) expressed as mass recovered / mass of licorice phytochemicals feed, total phenolic compounds content (TPC) expressed as GAE (mg of gallic acid equivalents/g), antioxidant activity expressed as TEAC (mmol Trolox equivalent/ml) and IC_{50} values (µg/ml). LES concentration = 14.2 mg/ml. $SCCO_2$ and LES flows were, respectively, 50 and 2 g/min. Precipitation time = 45 min.

SAS conditions			Precipitate (P)				Oleoresin (O)			
Exp.	**P / MPa**	**T / K**	**Yield %**	**TPC / mg/g**	**TEAC / mmol/ml**	**IC_{50} / µg/ml**	**Yield %**	**TPC / mg/g**	**TEAC / mmol/ml**	**IC_{50} / µg/ml**
1	15.0	313.15	13.28 ± 9.21	145.2 ± 3.4	0.690 ± 0.015	18.37 ± 0.73	41.35 ± 17.02	166.9 ± 3.2	0.484 ± 0.002	26.67 ± 0.16
2	20.0	313.15	23.48 ± 8.11	133.1 ± 1.8	0.709 ± 0.021	18.19 ± 0.40	34.75 ± 16.50	161.0 ± 5.1	0.524 ± 0.017	24.70 ± 0.55
3	12.5	308.15	33.42 ± 3.34	167.1 ± 9.4	0.760 ± 0.023	16.88 ± 0.25	25.23 ± 3.14	160.0 ± 10.6	0.483 ± 0.035	26.94 ± 2.06
4	15.0	308.15	33.93 ± 1.41	154.4 ± 11.4	0.764 ± 0.015	16.98 ± 0.09	30.40 ± 1.29	167.8 ± 5.1	0.511 ± 0.024	25.56 ± 1.33
5	17.5	308.15	28.64 ± 1.22	152.3 ± 11.1	0.711 ± 0.028	18.37 ± 1.13	38.66 ± 4.03	164.9 ± 3.9	0.487 ± 0.026	26.48 ± 1.32
6	20.0	308.15	28.77 ± 0.45	157.7 ± 3.1	0.697 ± 0.035	18.75 ± 1.15	37.89 ± 9.40	160.3 ± 23.9	0.481 ± 0.023	27.15 ± 1.09

Table 2. SAS conditions in the fractionation and precipitation of licorice ethanolic solution (LES). Yield (Y) expressed as mass recovered / mass of licorice phytochemicals feed, total phenolic compounds content (TPC) expressed as GAE (mg of gallic acid equivalents/g), antioxidant activity expressed as TEAC (mmol Trolox equivalent/ml) and IC_{50} values (µg/ml). LES concentration = 9.6 mg/ml. $SCCO_2$ and LES flows were, respectively, 50 and 2 g/min. Precipitation time = 45 min.

SAS conditions			Precipitate (P)				Oleoresin (O)			
Exp.	**P / MPa**	**T / K**	**Yield %**	**TPC / mg/g**	**TEAC / mmol/ml**	**IC_{50} / µg/ml**	**Yield %**	**TPC / mg/g**	**TEAC / mmol/ml**	**IC_{50} / µg/ml**
7	15	308.15	52.70	160.8 ± 3.2	0.734 ± 0.008	17.29 ± 0.59	38.25	160.3 ± 23.9	0.498 ± 0.003	26.00 ± 0.11
8	20	308.15	30.35	163.8 ± 4.8	0.776 ± 0.005	16.67 ± 0.08	37.62	168.9 ± 5.6	0.456 ± 0.006	27.89 ± 0.84
9	15	313.15	44.20	161.4 ± 3.5	0.721 ± 0.003	18.11 ± 0.31	36.63	150.2 ± 4.4	0.445 ± 0.002	28.81 ± 0.49
10	20	313.15	33.95	148.8 ± 7.3	0.733 ± 0.008	17.36 ± 0.54	56.63	177.8 ± 6.2	0.511 ± 0.016	25.28 ± 0.55

623 **Table 3.** Licorice bioactive compounds identified and quantified (mg/g) in SAS precipitates and oleoresins (HPLC-DAD analysis).

	Liquiritin	Liquiritigenin	Glycyrrhizic acid	Isoliquiritigenin	Glabridin
UAE extract	5.23 ± 0.01	0.73 ± 0.00	0.52 ± 0.17	0.63 ± 0.00	28.99 ± 2.13
(a) Precipitates					
1	8.34 ± 0.06	0.58 ± 0.02	0.32 ± 0.01	0.52 ± 0.00	12.75 ± 0.38
2	8.11 ± 0.07	0.32 ± 0.00	0.28 ± 0.00	0.46 ± 0.00	10.89 ± 0.03
3	9.12 ± 0.77	0.26*	0.40 ± 0.03	0.60 ± 0.01	23.29 ± 6.63
4	8.59 ± 0.34	0.57*	0.37 ± 0.04	0.56 ± 0.01	16.31 ± 0.74
5	8.92 ± 0.24	0.57 ± 0.18	0.43 ± 0.10	0.54 ± 0.01	16.26 ± 1.44
6	8.72 ± 0.25	0.56 ± 0.04	0.44 ± 0.05	0.52 ± 0.01	14.82 ± 1.76
7	8.84 ± 0.00	0.38 ± 0.00	0.42 ± 0.00	0.48 ± 0.00	12.66 ± 0.08
8	9.37 ± 0.01	0.44 ± 0.07	0.56 ± 0.16	0.47 ± 0.00	10.94 ± 1.77
9	8.05 ± 0.02	0.58 ± 0.00	0.39 ± 0.01	0.52 ± 0.00	12.53 ± 3.90
10	9.61 ± 0.11	0.56 ± 0.05	0.42 ± 0.00	0.50 ± 0.01	15.23 ± 5.40
(b) Oleoresins					
1	0.89 ± 0.00	0.89 ± 0.00	0.22 ± 0.00	0.81 ± 0.00	56.26 ± 1.59
2	0.71 ± 0.01	0.95 ± 0.00	0.25 ± 0.03	0.83 ± 0.01	51.90 ± 0.96
3	n. d.	0.87 ± 0.03	0.19 ± 0.01	0.79 ± 0.02	57.07 ± 0.99
4	0.74 ± 0.01	0.84 ± 0.02	0.18 ± 0.01	0.78 ± 0.01	54.70 ± 1.17
5	n. d.	1.02 ± 0.15	0.22 ± 0.03	0.87 ± 0.08	61.66 ± 8.00
6	n. d.	0.89 ± 0.09	0.22 ± 0.00	0.88 ± 0.06	54.562± 2.38
7	n. d.	1.00 ± 0.00	0.19 ± 0.00	0.84 ± 0.00	53.83 ± 0.20
8	0.72 ± 0.01	1.09 ± 0.29	0.23 ± 0.07	0.89 ± 0.14	57.67 ± 13.25
9	n. d.	0.73 ± 0.05	0.18 ± 0.08	0.72 ± 0.02	55.11 ± 4.56
10	n. d.	1.13 ± 0.11	0.21 ± 0.01	0.93 ± 0.05	62.53 ± 5.47

624 n.d.: non detected

625 * No duplicate available

626 **Table 4.** Mean particle size and size distributions of SAS particles in the precipitates.

Exp.	P / MPa	T / K	d (0,1) (μm)	d (0,5) (μm)	d (0,9) (μm)	Mean diameter (μm)
1	15.0	313.15	7.04	35.19	71.78	37.90
2	20.0	313.15	10.65	34.16	61.87	35.82
3	12.5	308.15	5.66	30.57	68.05	34.27
4	15.0	308.15	7.35	36.94	71.54	39.09
5	17.5	308.15	3.82	20.20	48.82	23.58
6	20.0	308.15	4.12	17.15	41.52	20.32
7	15	308.15	3.69	13.43	34.07	16.51
8	20	308.15	3.91	14.58	39.25	18.55
9	15	313.15	3.15	9.74	25.85	12.54
10	20	313.15	2.73	8.01	23.72	10.94

627

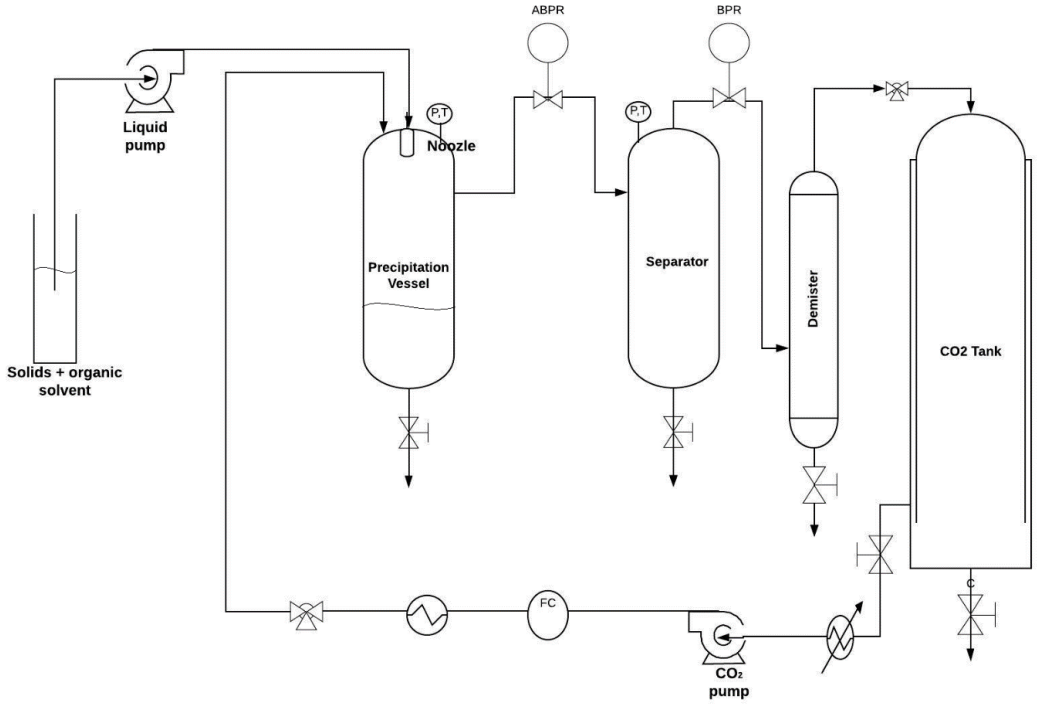

628

629 **Figure 1.** Schematic diagram of the SAS process. ABPR: Automatic back pressure
630 regulator, BPR: manual back pressure regulator, P: manometer, T: temperature probe,
631 FC: flowmeter.

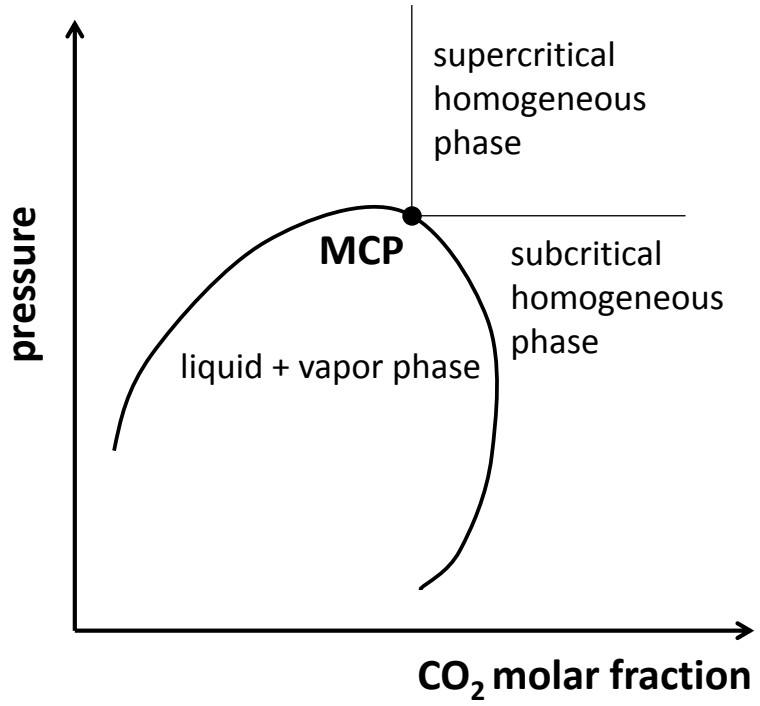

632

633 **Figure 2.** Scheme of the pressure vs. composition phase diagram of the binary mixture
634 of $SCCO_2$ + ethanol. MCP: mixture critical point.

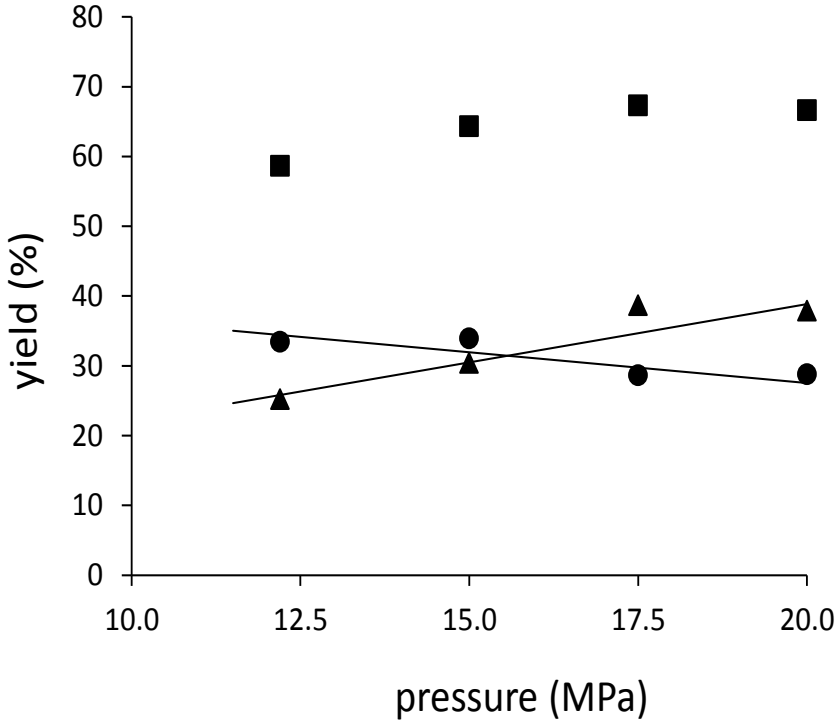

635

636 **Figure 3.** Precipitate (●), oleoresin, (▲) and total (precipitate + oleoresin) (■) yields
637 as a function of SAS precipitation pressure, corresponding to experiments 3 to 6 of
638 Table 1 (308.15 K and LES concentration of 14.2 mg/ml). (——) Trend line.

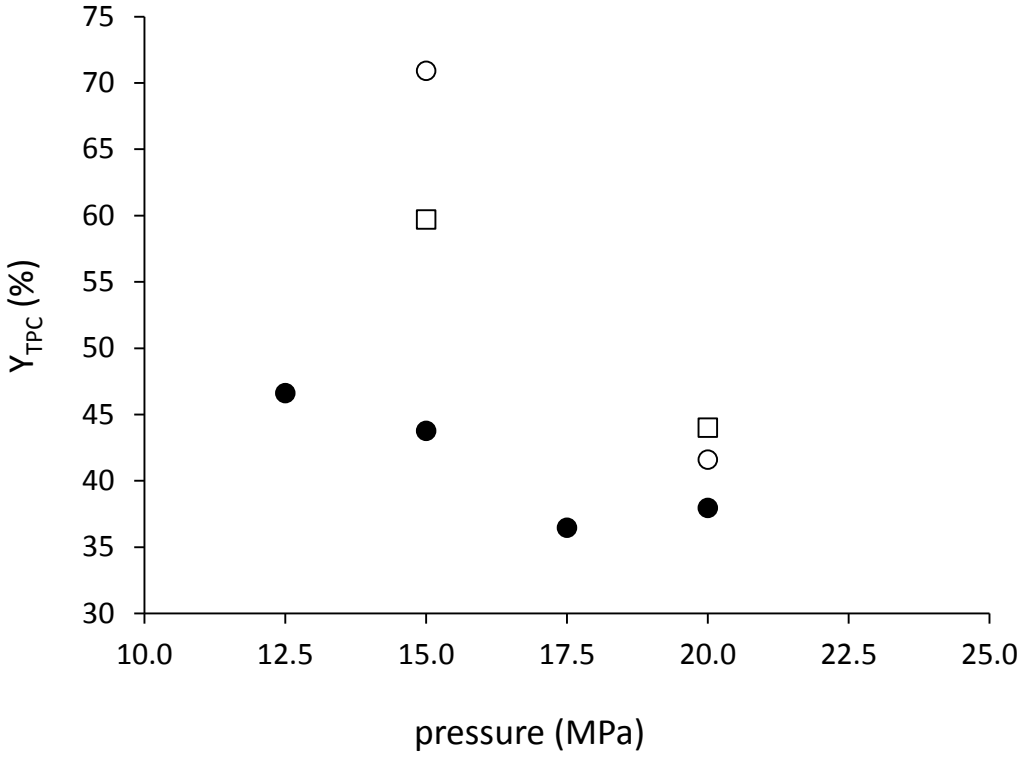

639

640 **Figure 4.** Recovery of TPC (Y_{TPC}) in precipitates as a function of SAS pressure and
641 concentration of phytochemicals in the licorice ethanolic solution. (●) LES1 (14.2
642 mg/ml) and 308.15 K; (○) LES2 (9.6 mg/ml) and 308 K; (□) LES2 (9.6 mg/ml) and
643 313.15 K.

(a)

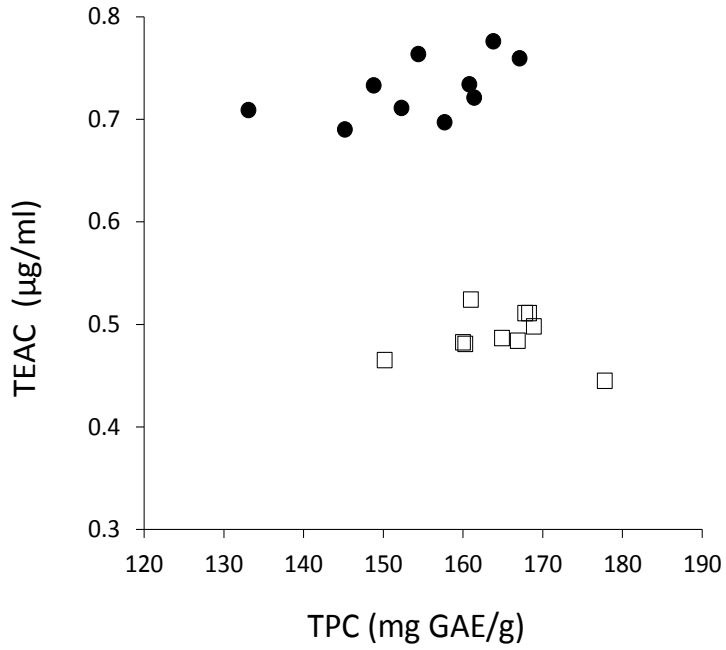

(b)

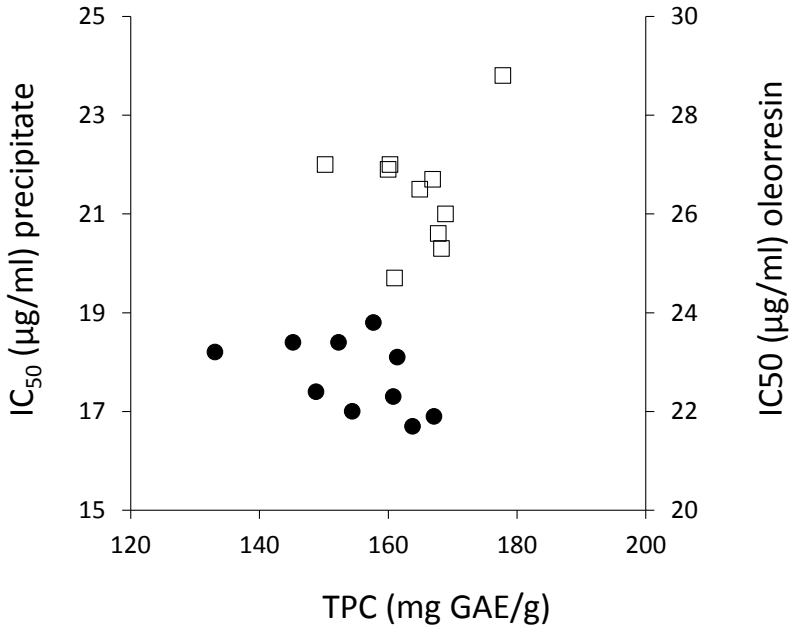

644 **Figure 5.** (a) TEAC values and (b) IC_{50} values of (●) precipitates and (□) oleoresins as
645 a function of total phenolic compounds (TPC, mg GAE/g).

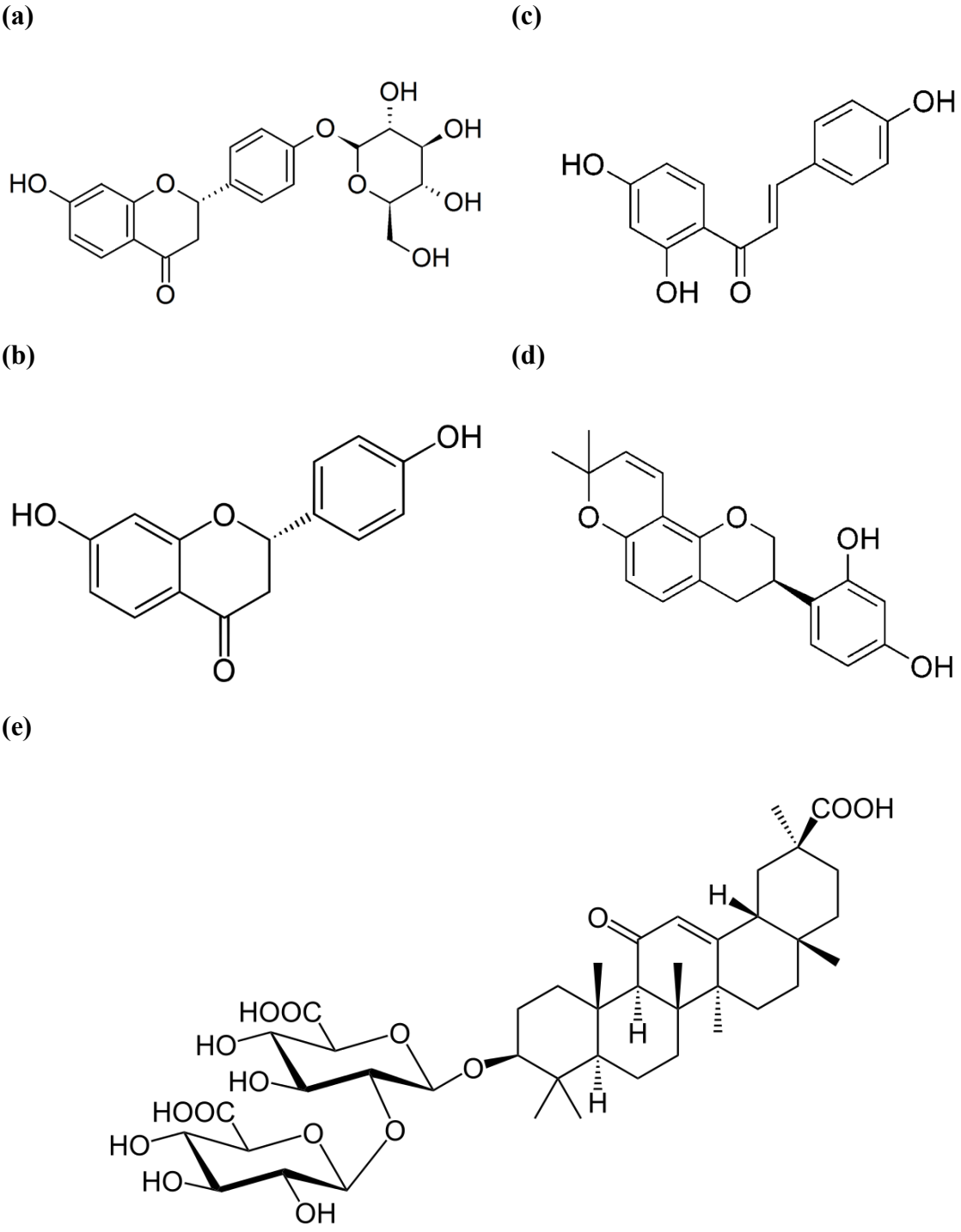

646 **Figure 6.** Chemical structure of (A) liquiritin, (B) liquiritigenin, (C) isoliquiritigenin
647 and (D) glabridin and (E) glycyrrhizic acid.

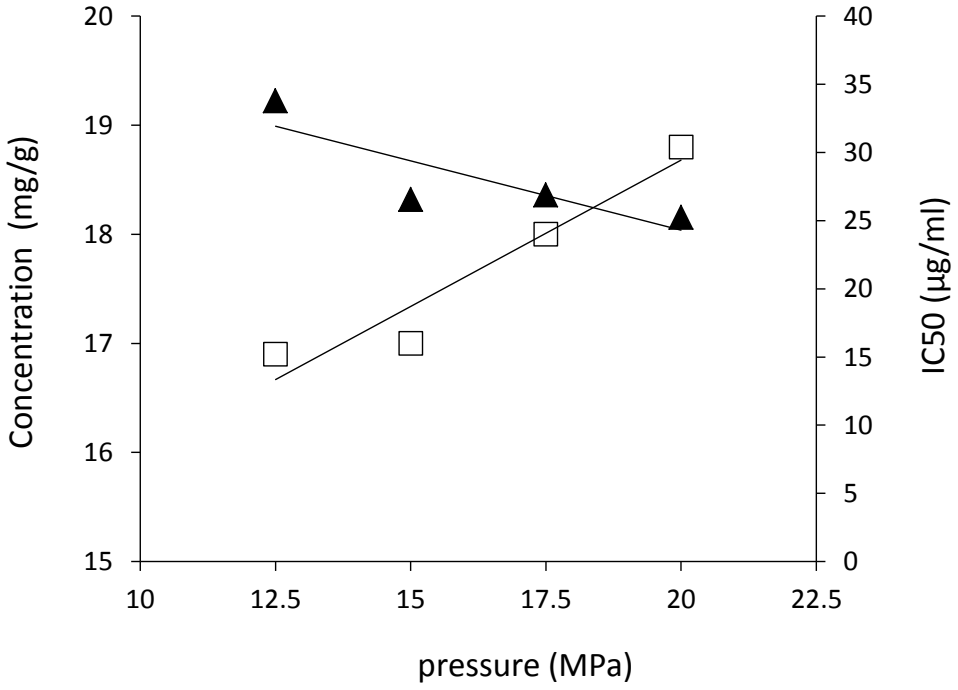

Figure 7. (□) IC_{50} values and (▲) sum of the concentration of key licorice bioactive compounds (Table 3) as a function of pressure at 308.15 K and 14.2 mg/ml LES.

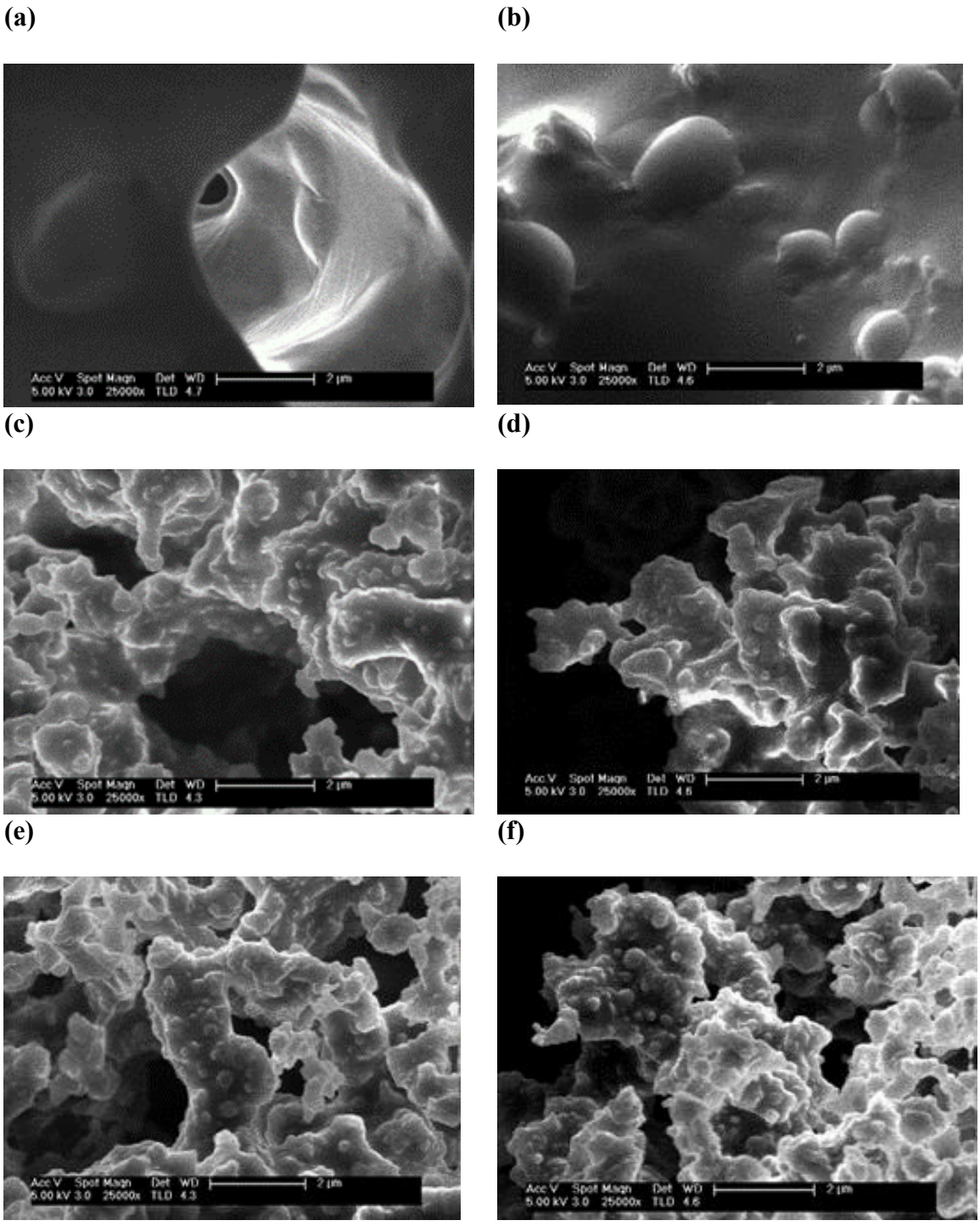

651 **Figure 8.** SEM images (25000 x) of precipitates obtained with LES1 (14.2 mg/ml): (a)
652 to (f), experiments 1 to 6 in Table 1.

(a) **(b)**

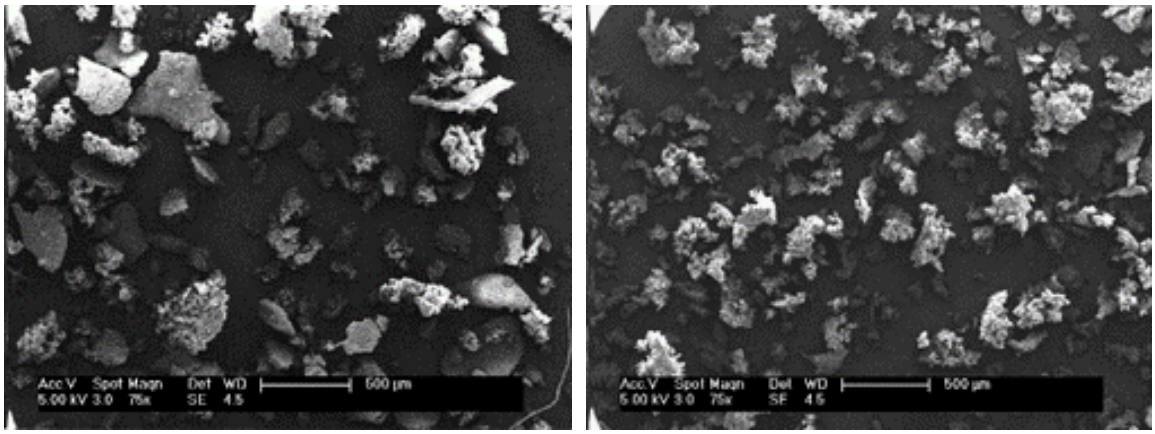

653 **Figure 9.** SEM imagens (75x) of precipitates obtained at 313 K with LES1 (14.2
654 mg/ml): (a) experiment 1 and (b) experiment 2 of Table 1.

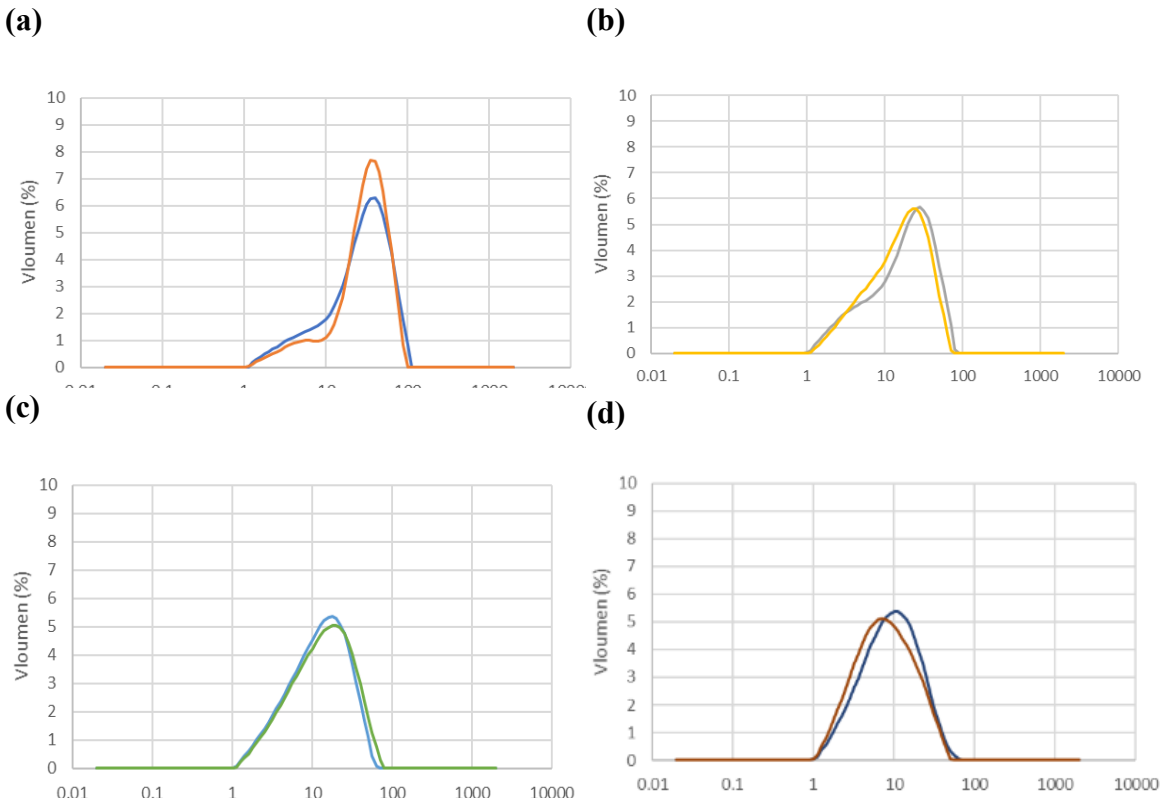

Figure 10. Particle size distribution (µm) of precipitates obtained at 308.15 K with LES1 (14.2 mg/g). Duplicate experiments 3 to 6 of Table 1: (a) 12.5 MPa; (b) 15 MPa; (c) 17.5 MPa; (d) 20 MPa.

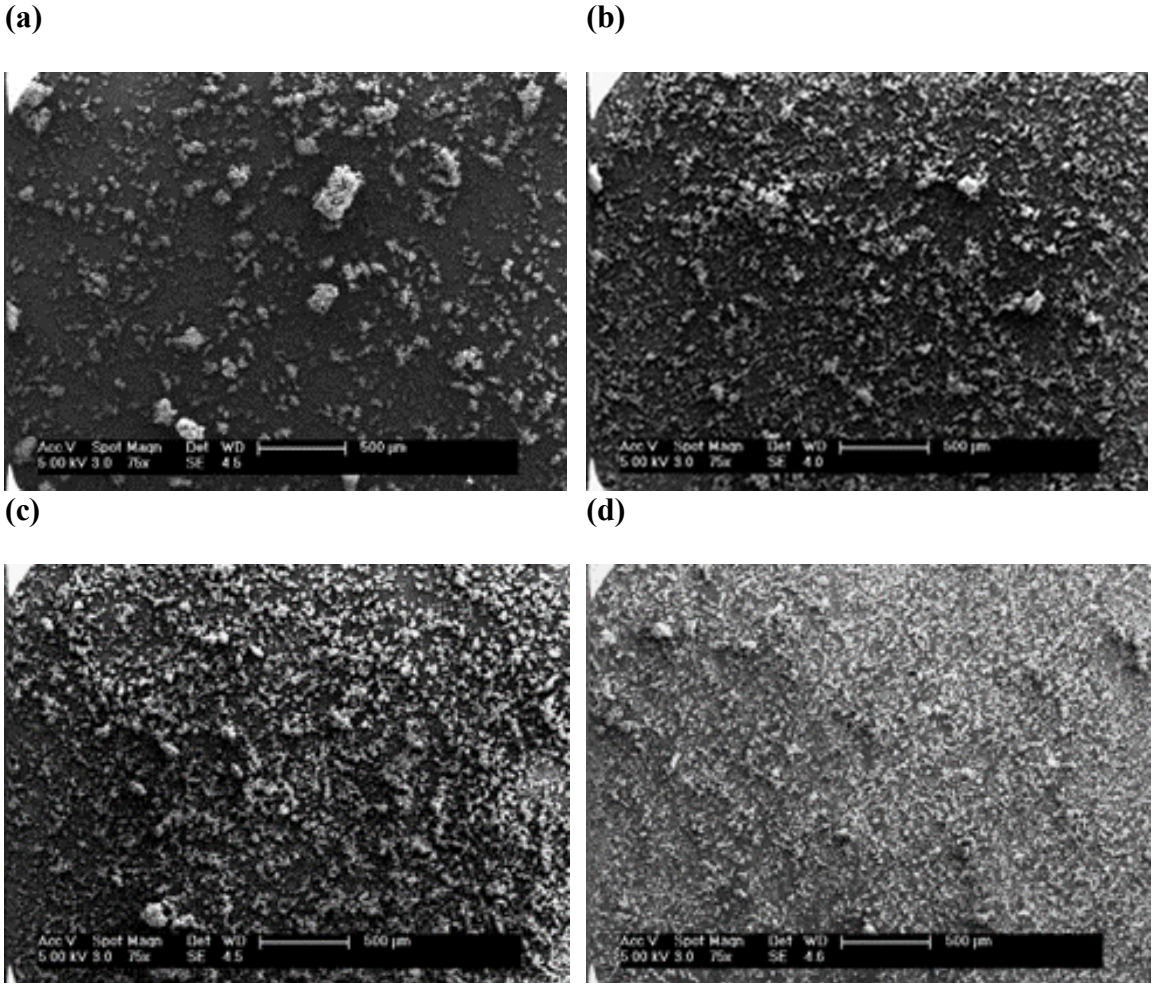

659 **Figure 11.** SEM imagens (75x) for precipitates at 308.15 K: (a) 15 MPa and 14.2
660 mg/ml (LES1); (b) 15 MPa and 9.6 mg/ml (LES2); (c) 20 MPa and 14.2 mg/ml (LES1);
661 (d) 20 MPa and 9.6 mg/ml (LES2).

Table 1. SAS conditions in the fractionation and precipitation of licorice ethanolic solution (LES). Yield (Y) expressed as mass recovered / mass of licorice phytochemicals feed, total phenolic compounds content (TPC) expressed as GAE (mg of gallic acid equivalents/g), antioxidant activity expressed as TEAC (mmol Trolox equivalent/ml) and IC_{50} values (µg/ml). LES concentration = 14.2 mg/ml. $SCCO_2$ and LES flows were, respectively, 50 and 2 g/min. Precipitation time = 45 min.

SAS conditions			Precipitate (P)				Oleoresin (O)			
Exp.	P / MPa	T / K	Yield %	TPC / mg/g	TEAC / mmol/ml	IC_{50} / µg/ml	Yield %	TPC / mg/g	TEAC / mmol/ml	IC_{50} / µg/ml
1	15.0	313.15	13.28 ± 9.21	145.2 ± 3.4	0.690 ± 0.015	18.37 ± 0.73	41.35 ± 17.02	166.9 ± 3.2	0.484 ± 0.002	26.67 ± 0.16
2	20.0	313.15	23.48 ± 8.11	133.1 ± 1.8	0.709 ± 0.021	18.19 ± 0.40	34.75 ± 16.50	161.0 ± 5.1	0.524 ± 0.017	24.70 ± 0.55
3	12.5	308.15	33.42 ± 3.34	167.1 ± 9.4	0.760 ± 0.023	16.88 ± 0.25	25.23 ± 3.14	160.0 ± 10.6	0.483 ± 0.035	26.94 ± 2.06
4	15.0	308.15	33.93 ± 1.41	154.4 ± 11.4	0.764 ± 0.015	16.98 ± 0.09	30.40 ± 1.29	167.8 ± 5.1	0.511 ± 0.024	25.56 ± 1.33
5	17.5	308.15	28.64 ± 1.22	152.3 ± 11.1	0.711 ± 0.028	18.37 ± 1.13	38.66 ± 4.03	164.9 ± 3.9	0.487 ± 0.026	26.48 ± 1.32
6	20.0	308.15	28.77 ± 0.45	157.7 ± 3.1	0.697 ± 0.035	18.75 ± 1.15	37.89 ± 9.40	160.3 ± 23.9	0.481 ± 0.023	27.15 ± 1.09

Table 2. SAS conditions in the fractionation and precipitation of licorice ethanolic solution (LES). Yield (Y) expressed as mass recovered / mass of licorice phytochemicals feed, total phenolic compounds content (TPC) expressed as GAE (mg of gallic acid equivalents/g), antioxidant activity expressed as TEAC (mmol Trolox equivalent/ml) and IC_{50} values (µg/ml). LES concentration = 9.6 mg/ml. $SCCO_2$ and LES flows were, respectively, 50 and 2 g/min. Precipitation time = 45 min.

SAS conditions			**Precipitate (P)**				**Oleoresin (O)**			
Exp.	**P / MPa**	**T / K**	**Yield %**	**TPC / mg/g**	**TEAC / mmol/ml**	**IC_{50} / µg/ml**	**Yield %**	**TPC / mg/g**	**TEAC / mmol/ml**	**IC_{50} / µg/ml**
7	15	308.15	52.70	160.8 ± 3.2	0.734 ± 0.008	17.29 ± 0.59	38.25	160.3 ± 23.9	0.498 ± 0.003	26.00 ± 0.11
8	20	308.15	30.35	163.8 ± 4.8	0.776 ± 0.005	16.67 ± 0.08	37.62	168.9 ± 5.6	0.456 ± 0.006	27.89 ± 0.84
9	15	313.15	44.20	161.4 ± 3.5	0.721 ± 0.003	18.11 ± 0.31	36.63	150.2 ± 4.4	0.445 ± 0.002	28.81 ± 0.49
10	20	313.15	33.95	148.8 ± 7.3	0.733 ± 0.008	17.36 ± 0.54	56.63	177.8 ± 6.2	0.511 ± 0.016	25.28 ± 0.55

Table 3. Licorice bioactive compounds identified and quantified (mg/g) in SAS precipitates and oleoresins (HPLC-DAD analysis).

	Liquiritin	Liquiritigenin	Glycyrrhizic acid	Isoliquiritigenin	Glabridin
UAE extract	5.23 ± 0.01	0.73 ± 0.00	0.52 ± 0.17	0.63 ± 0.00	28.99 ± 2.13
(a) Precipitates					
1	8.34 ± 0.06	0.58 ± 0.02	0.32 ± 0.01	0.52 ± 0.00	12.75 ± 0.38
2	8.11 ± 0.07	0.32 ± 0.00	0.28 ± 0.00	0.46 ± 0.00	10.89 ± 0.03
3	9.12 ± 0.77	0.26*	0.40 ± 0.03	0.60 ± 0.01	23.29 ± 6.63
4	8.59 ± 0.34	0.57*	0.37 ± 0.04	0.56 ± 0.01	16.31 ± 0.74
5	8.92 ± 0.24	0.57 ± 0.18	0.43 ± 0.10	0.54 ± 0.01	16.26 ± 1.44
6	8.72 ± 0.25	0.56 ± 0.04	0.44 ± 0.05	0.52 ± 0.01	14.82 ± 1.76
7	8.84 ± 0.00	0.38 ± 0.00	0.42 ± 0.00	0.48 ± 0.00	12.66 ± 0.08
8	9.37 ± 0.01	0.44 ± 0.07	0.56 ± 0.16	0.47 ± 0.00	10.94 ± 1.77
9	8.05 ± 0.02	0.58 ± 0.00	0.39 ± 0.01	0.52 ± 0.00	12.53 ± 3.90
10	9.61 ± 0.11	0.56 ± 0.05	0.42 ± 0.00	0.50 ± 0.01	15.23 ± 5.40
(b) Oleoresins					
1	0.89 ± 0.00	0.89 ± 0.00	0.22 ± 0.00	0.81 ± 0.00	56.26 ± 1.59
2	0.71 ± 0.01	0.95 ± 0.00	0.25 ± 0.03	0.83 ± 0.01	51.90 ± 0.96
3	n. d.	0.87 ± 0.03	0.19 ± 0.01	0.79 ± 0.02	57.07 ± 0.99
4	0.74 ± 0.01	0.84 ± 0.02	0.18 ± 0.01	0.78 ± 0.01	54.70 ± 1.17
5	n. d.	1.02 ± 0.15	0.22 ± 0.03	0.87 ± 0.08	61.66 ± 8.00
6	n. d.	0.89 ± 0.09	0.22 ± 0.00	0.88 ± 0.06	54.562± 2.38
7	n. d.	1.00 ± 0.00	0.19 ± 0.00	0.84 ± 0.00	53.83 ± 0.20
8	0.72 ± 0.01	1.09 ± 0.29	0.23 ± 0.07	0.89 ± 0.14	57.67 ± 13.25
9	n. d.	0.73 ± 0.05	0.18 ± 0.08	0.72 ± 0.02	55.11 ± 4.56
10	n. d.	1.13 ± 0.11	0.21 ± 0.01	0.93 ± 0.05	62.53 ± 5.47

n.d.: non detected

* No duplicate available

Table 4. Mean particle size and size distributions of SAS particles in the precipitates.

Exp.	P / MPa	T / K	d (0,1) (µm)	d (0,5) (µm)	d (0,9) (µm)	Mean diameter (µm)
1	15.0	313.15	7.04	35.19	71.78	37.90
2	20.0	313.15	10.65	34.16	61.87	35.82
3	12.5	308.15	5.66	30.57	68.05	34.27
4	15.0	308.15	7.35	36.94	71.54	39.09
5	17.5	308.15	3.82	20.20	48.82	23.58
6	20.0	308.15	4.12	17.15	41.52	20.32
7	15	308.15	3.69	13.43	34.07	16.51
8	20	308.15	3.91	14.58	39.25	18.55
9	15	313.15	3.15	9.74	25.85	12.54
10	20	313.15	2.73	8.01	23.72	10.94

Figure

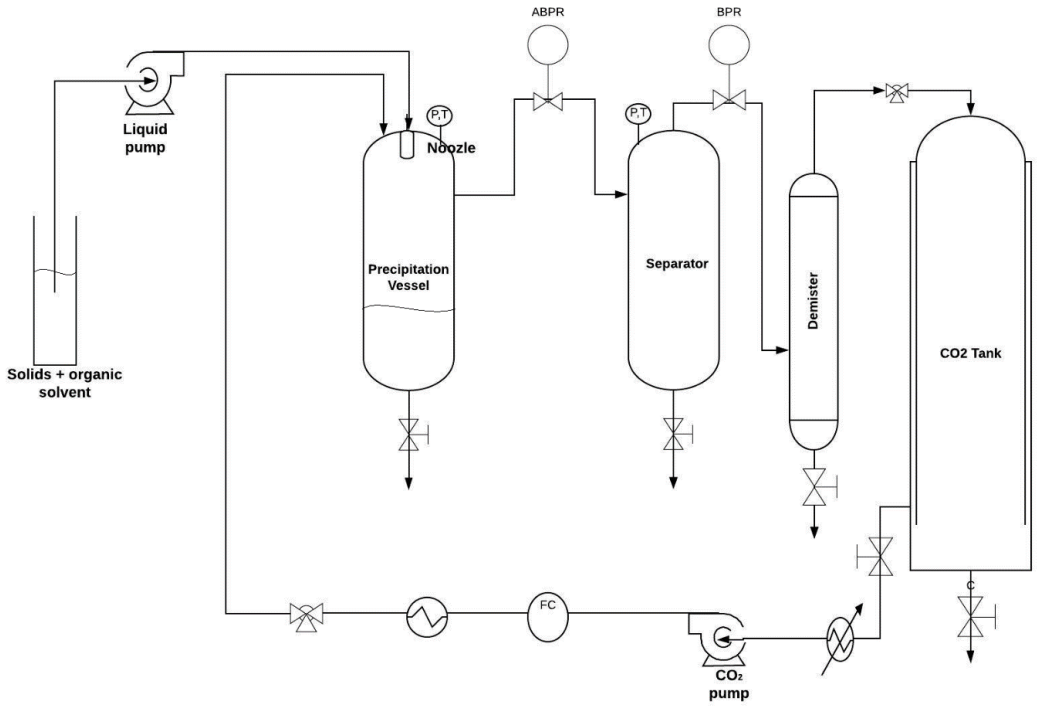

Figure 1. Schematic diagram of the SAS process. ABPR: Automatic back pressure regulator, BPR: manual back pressure regulator, P: manometer, T: temperature probe, FC: flowmeter.

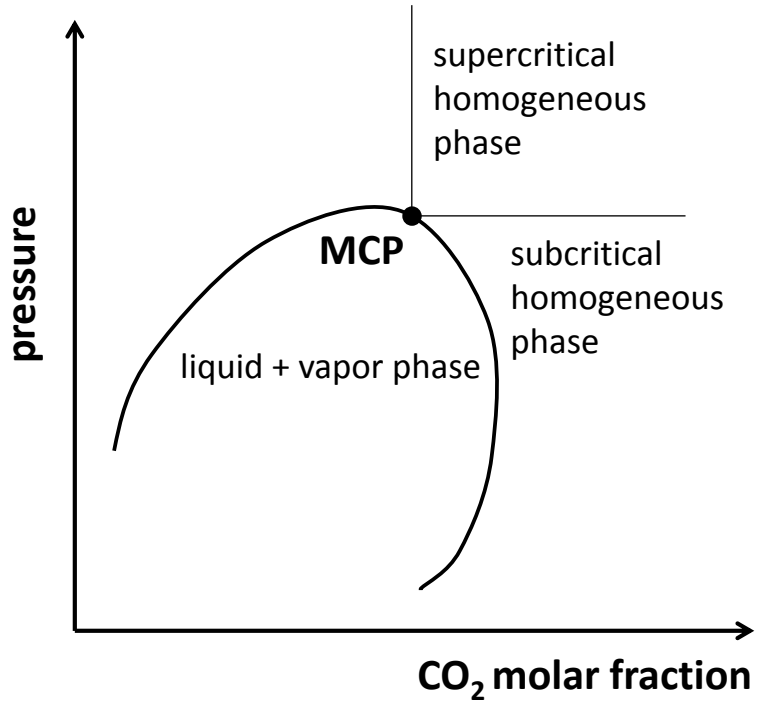

Figure 2. Scheme of the pressure vs. composition phase diagram of the binary mixture of $SCCO_2$ + ethanol. MCP: mixture critical point.

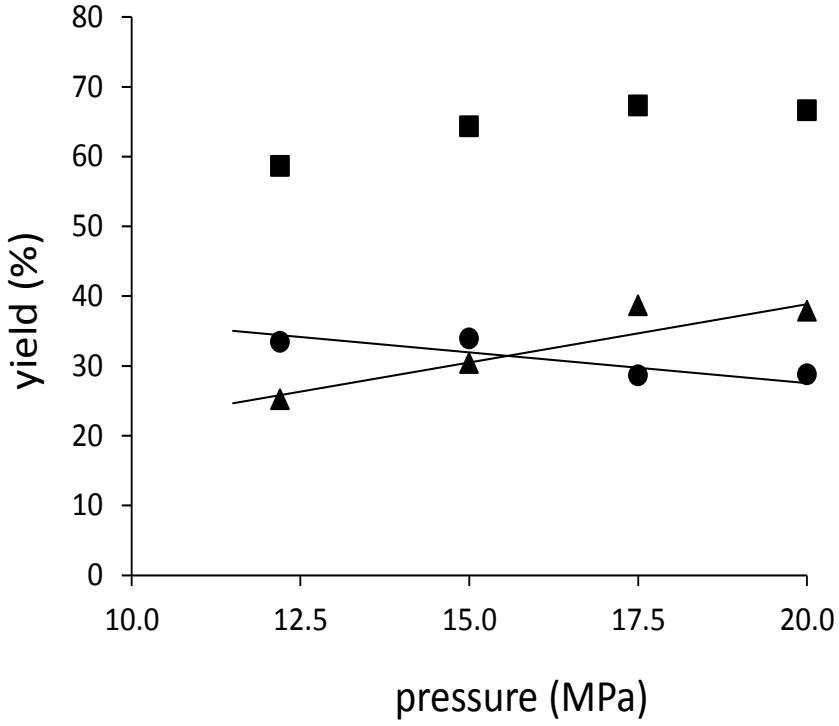

Figure 3. Precipitate (●), oleoresin, (▲) and total (precipitate + oleoresin) (■) yields as a function of SAS precipitation pressure, corresponding to experiments 3 to 6 of Table 1 (308.15 K and LES concentration of 14.2 mg/ml). (——) Trend line.

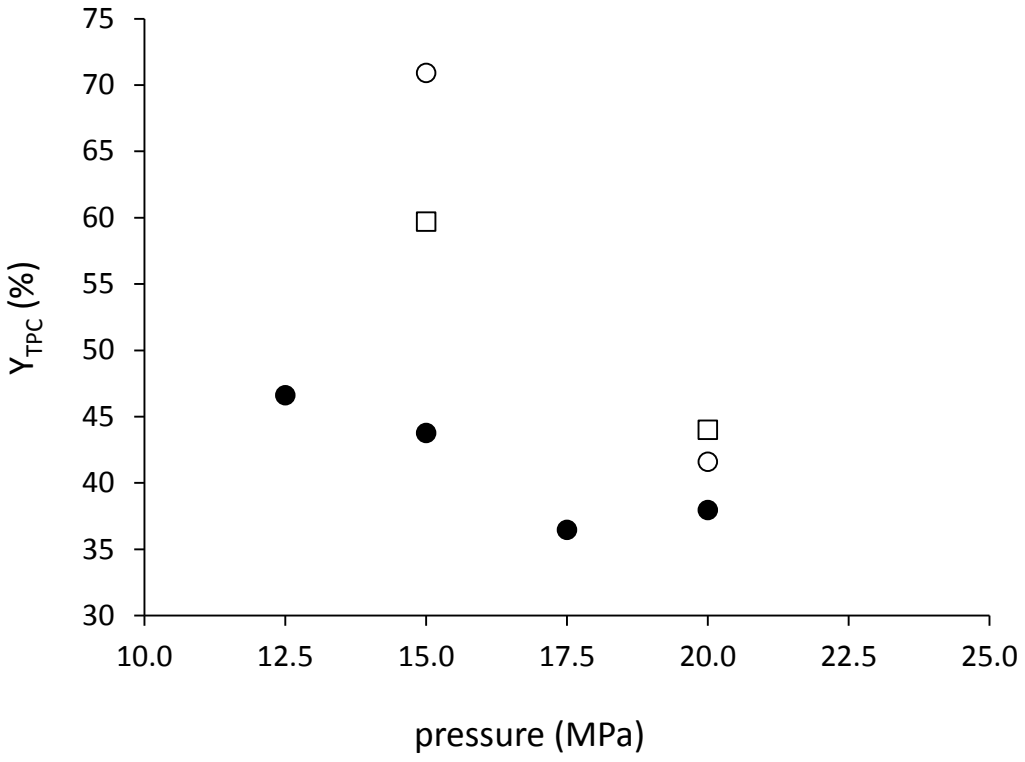

Figure 4. Recovery of TPC (Y_{TPC}) in precipitates as a function of SAS pressure and concentration of phytochemicals in the licorice ethanolic solution. (●) LES1 (14.2 mg/ml) and 308.15 K; (○) LES2 (9.6 mg/ml) and 308 K; (□) LES2 (9.6 mg/ml) and 313.15 K.

(a)

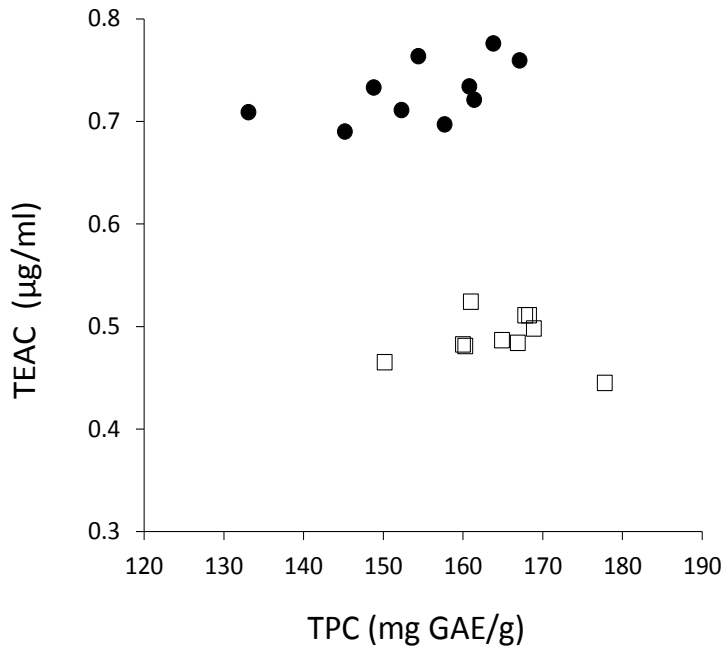

(b)

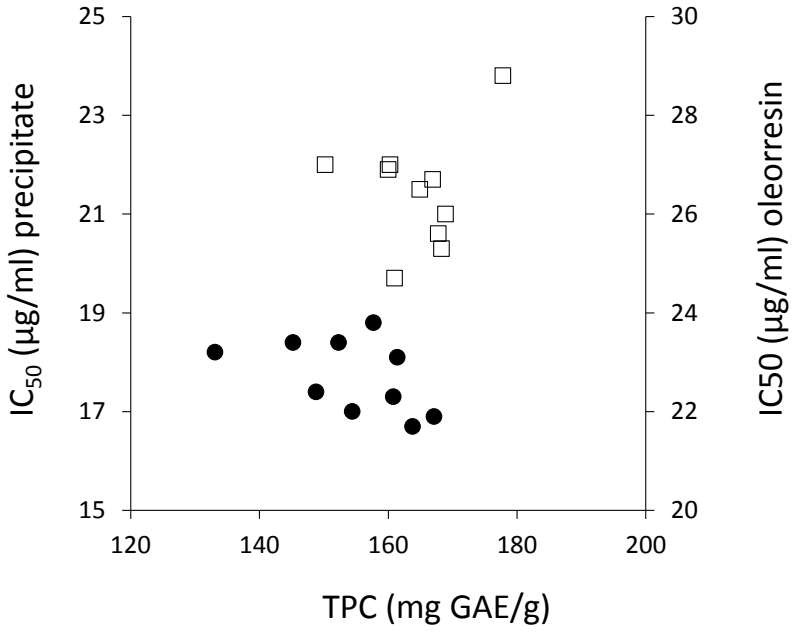

Figure 5. (a) TEAC values and (b) IC_{50} values of (●) precipitates and (□) oleoresins as a function of total phenolic compounds (TPC, mg GAE/g).

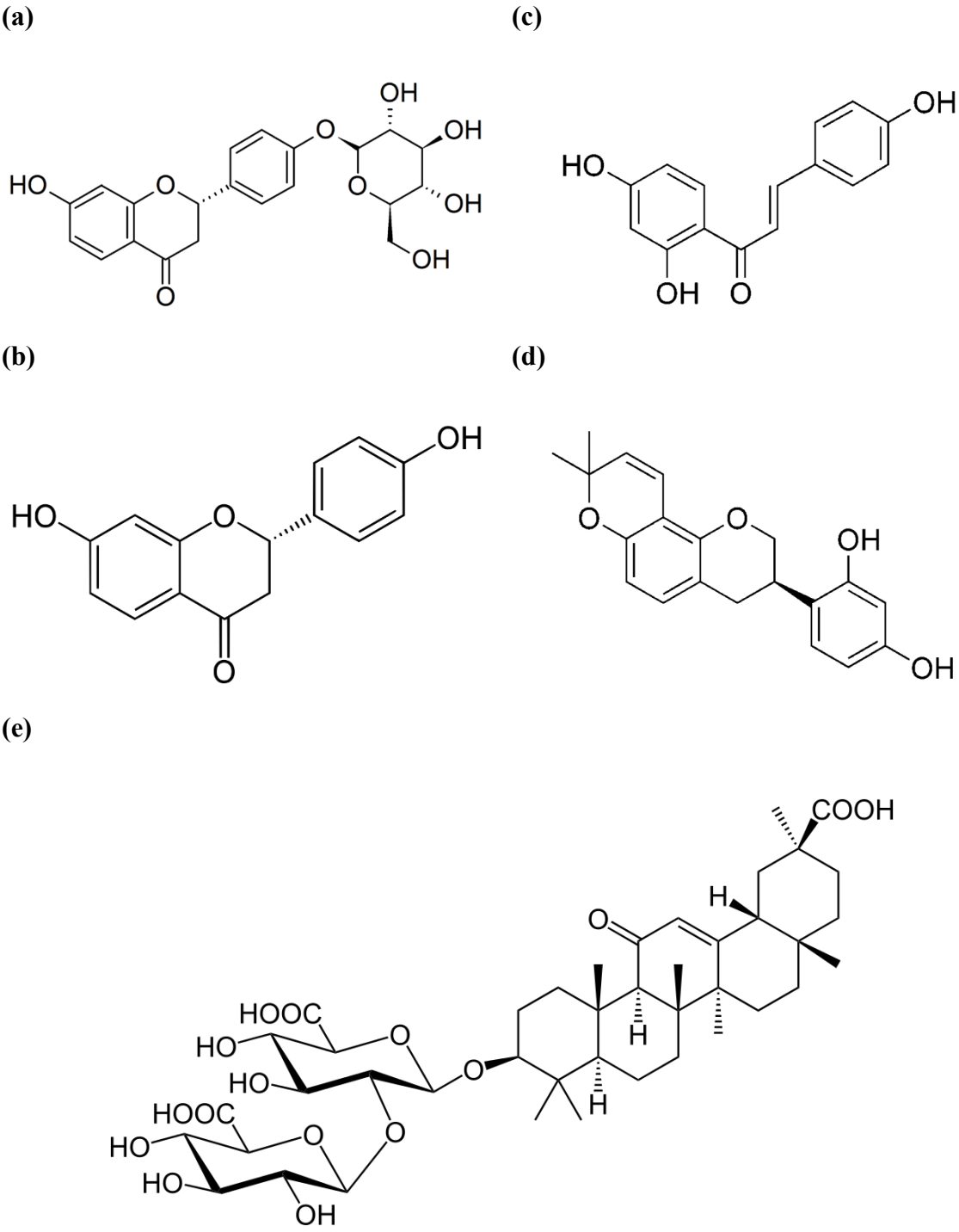

Figure 6. Chemical structure of (A) liquiritin, (B) liquiritigenin, (C) isoliquiritigenin and (D) glabridin and (E) glycyrrhizic acid.

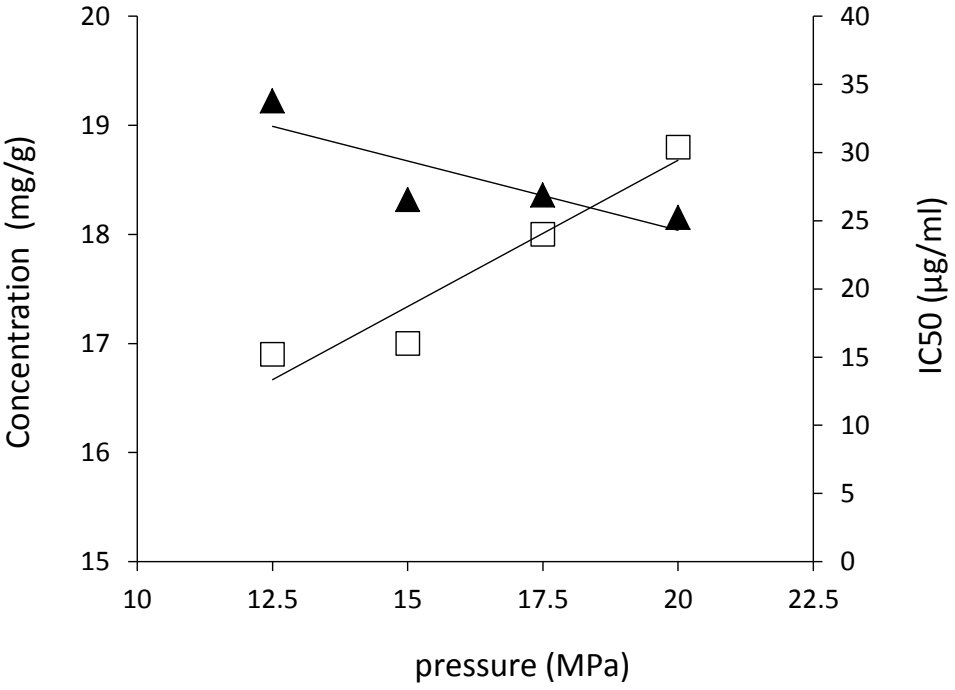

Figure 7. (□) IC_{50} values and (▲) sum of the concentration of key licorice bioactive compounds (Table 3) as a function of pressure at 308.15 K and 14.2 mg/ml LES.

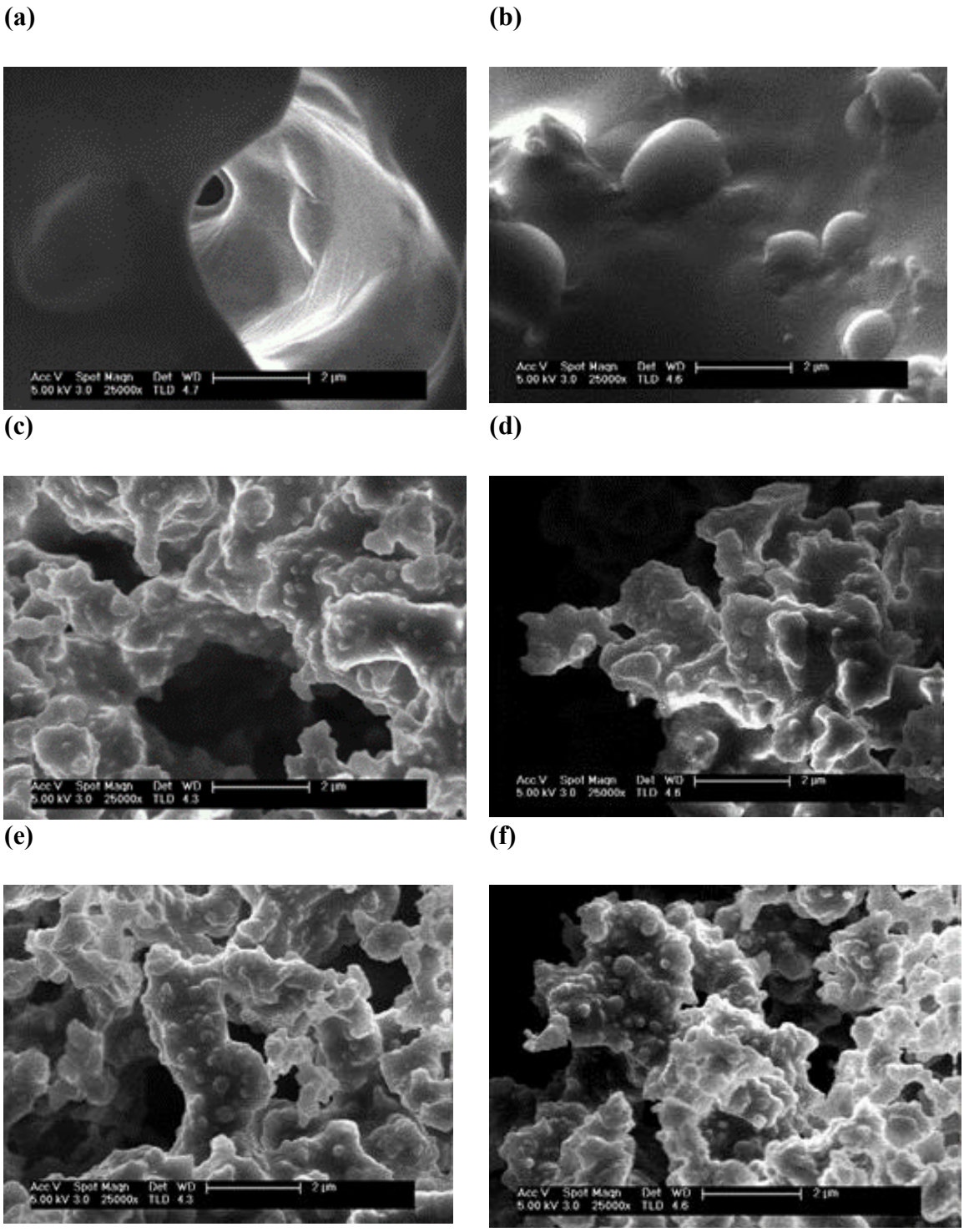

Figure 8. SEM images (25000 x) of precipitates obtained with LES1 (14.2 mg/ml): (a) to (f), experiments 1 to 6 in Table 1.

(a) **(b)**

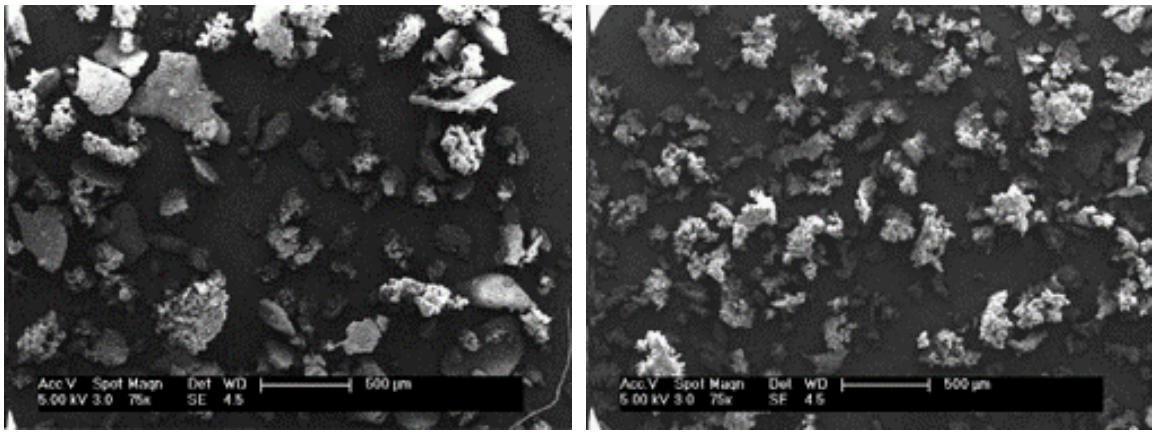

Figure 9. SEM imagens (75x) of precipitates obtained at 313 K with LES1 (14.2 mg/ml): (a) experiment 1 and (b) experiment 2 of Table 1.

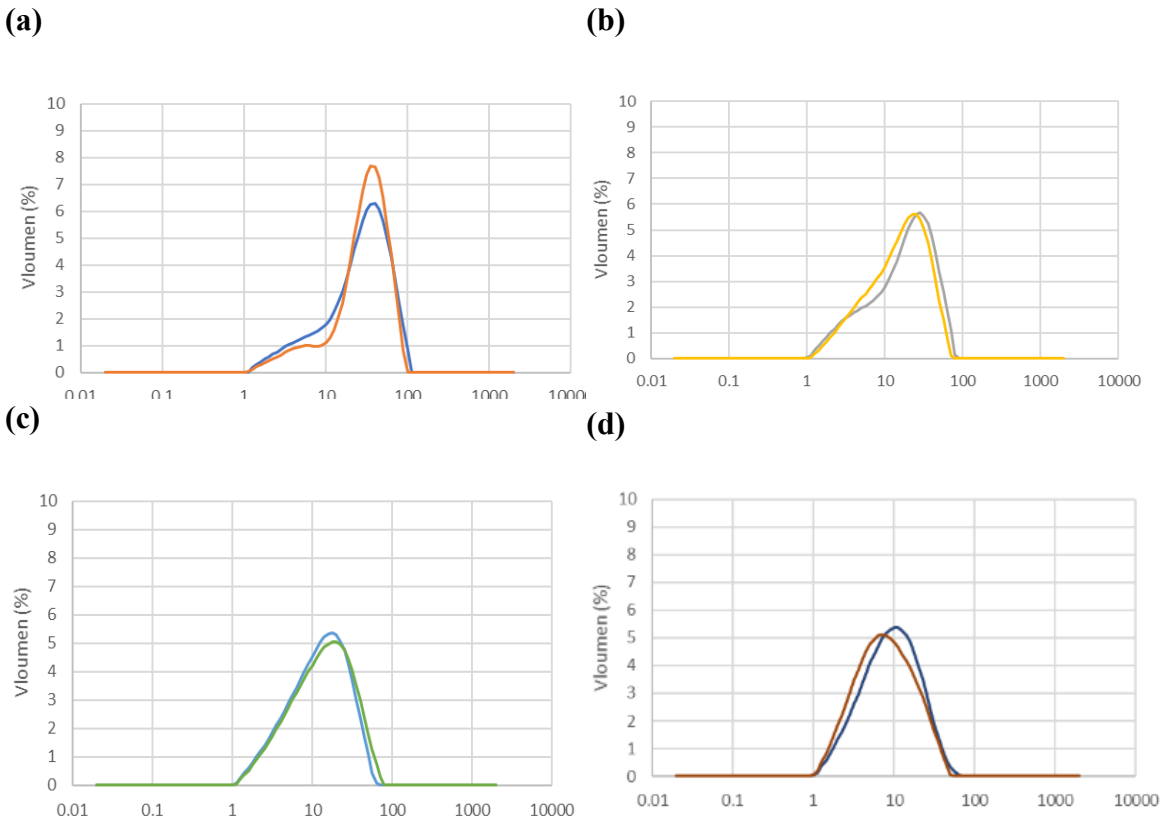

Figure 10. Particle size distribution (μm) of precipitates obtained at 308.15 K with LES1 (14.2 mg/g). Duplicate experiments 3 to 6 of Table 1: (a) 12.5 MPa; (b) 15 MPa; (c) 17.5 MPa; (d) 20 MPa.

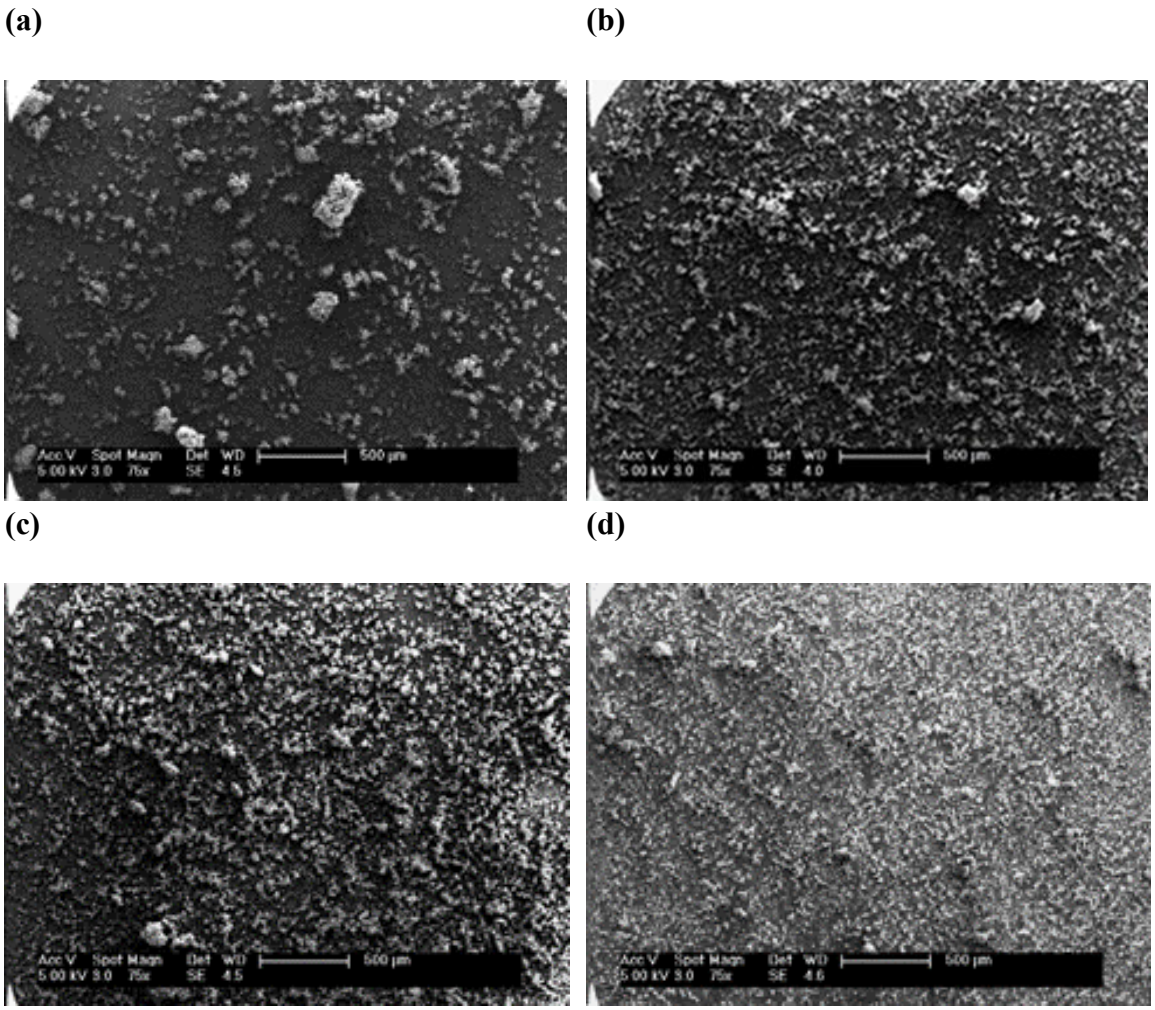

Figure 11. SEM imagens (75x) for precipitates at 308.15 K: (a) 15 MPa and 14.2 mg/ml (LES1); (b) 15 MPa and 9.6 mg/ml (LES2); (c) 20 MPa and 14.2 mg/ml (LES1); (d) 20 MPa and 9.6 mg/ml (LES2).

Fractionation and precipitation of licorice (*Glycyrrhiza glabra* L.) phytochemicals by supercritical antisolvent (SAS) technique

Somaris E. Quintana*, Diego Martín Hernández, David Villanueva-Bermejo, Mónica R. García-Risco, Tiziana Fornari

Institute of Food Science Research (CIAL), CEI UAM+CSIC, Madrid, Spain

Corresponding author: Somaris E. Quintana. Institute of Food Science Research (CIAL), CEI UAM+CSIC, Madrid, Spain. Phone: +34 910 017 976.

e-mail: somaris.quintana@predoc.uam.es

Abstract

The incorporation of bioactive compounds in food matrices is a priority field of current research in the area of food, nutrition and health. More efficient and environmentally clean technologies, such as supercritical fluid technology, are being studied and developed to achieve this goal. Supercritical anti-solvent precipitation using carbon dioxide constitutes one of these techniques and allows obtaining powdered food ingredients in the form of small size particles, facilitating their incorporation into food matrices and, in addition, increasing the bioavailability of the bioactive compounds. In this work the SAS precipitation of licorice phytochemicals was carried out.

The SAS precipitation of an ethanolic extract of licorice root, obtained by ultrasonic assisted extraction. The products obtained were studied concerning their antioxidant capacity, content of bioactive compounds (liquiritin, liquiritigenin, isoliquiritigenin, glabridin and glycyrrhizic acid), as well as the size and morphology of the particles obtained. SAS technique allows the fractionation of the phytochemicals contained in the ethanolic extract, increasing the antioxidant activity of the precipitates in comparison to that of the original extract. Additionally, it was established the influence of operating conditions to obtain dry, regular and small particles, with an average size of 16 μm under the optimal conditions assessed.

Keywords: Supercritical antisolvent precipitation; Licorice; Antioxidant activity; Morphology; Particle size distribution.

1. Introduction

Licorice (*Glycyrrhiza glabra* L.) grows in Mediterranean countries, Asia and Southeast Europe (Saxena, 2005). Due to its sweet flavor and bioactive properties, licorice was used as a medicinal plant. Studies have shown different properties as antitussive, antiulcer, antimicrobial and antiviral, thrombin inhibitor, anti-inflammatory, antidiabetic, hepato-protective and anticancer. These activities were related to the presence of triterpenoid-type and phenolic-type compounds, mainly liquiritin, liquiritigenin, glycyrrhizic acid, isoliquiritigenin and glabridin (Chin et al., 2007; Kaur, Kaur, & Dhindsa, 2013). Extraction techniques like ultrasound assisted extraction (Pan, Liu, Jia, & Shu, 2000), maceration (Sankeshwari, Ankola, Bhat, & Hullatti, 2018), pressurized liquid extraction (Baek, Lee, & Lee, 2008) or supercritical carbon dioxide extraction (Hedayati & Ghoreishi, 2015; Quintana et al., 2019), were investigated to improve the extraction of licorice bioactive constituents.

Natural extracts are in the market in liquid form, as oily preparations, or in solid form as powders. Dried powdered extracts have some advantages over liquid extracts, as higher concentration and stability of the bioactive substances together with lower storage costs (Visentin, Rodríguez-Rojo, Navarrete, Maestri, & Cocero, 2012). Powders containing micro- and/or nano-particles allow a better incorporation of bioactive substances in complex food matrices. Furthermore, smaller sizes improve the bioavailability of bioactive ingredients, increasing absorption and effectiveness (Martín & Cocero, 2008).

Traditionally, size reduction methods were based on physical techniques such as grinding, milling, crystallization or crushing, but these techniques do not allow small enough sizes (Rasenack & Müller, 2004). Nowadays, different techniques have been studied and developed to obtain powdered extracts with small particles, such as spray drying, spray cooling, lyophilization, liquid antisolvent precipitation, among others (X. Chang, Bao, Shan, Bao, & Pan, 2017; Lee et al., 2016; Morita, Horikiri, Suzuki, & Yoshino, 2001). In this respect, the micronization using supercritical fluids has some advantages, such as the possibility of obtaining particles with more homogeneous morphology, narrow particle size distribution (PSD), avoiding the thermal degradation of the product and reducing the use of liquid solvents (Wang, Liu, Wu, & Jiang, 2013).

SAS precipitation is based on the continuous contact between supercritical carbon dioxide ($SCCO_2$) and an organic solvent (highly soluble in $SCCO_2$) containing the targeted bioactive compounds. The solution is introduced in the precipitation vessel through a nozzle, forming small drops. The $SCCO_2$ penetrate in the droplets, inducing the solution supersaturation, followed by the bioactive substance precipitation (anti-solvent effect) into small solid and dry particles (Langa et al., 2019; Martín & Cocero, 2008). SAS precipitation conditions should ensure the complete removal of the organic solvent from the precipitation vessel (Reverchon, Torino, Dowy, Braeuer, & Leipertz, 2010). Therefore, the operating conditions depend largely on the solvent used (De Marco, Knauer, Cice, Braeuer, & Reverchon, 2012), and specifically on the phase equilibria of the CO_2 + solvent mixture. Thus, to achieve a satisfactory precipitation in SAS method, it is necessary to establish operating conditions above the CO_2 + solvent mixture critical point (MCP) to attain a homogeneous supercritical phase (De Marco et al., 2012; Reverchon, Adami, Caputo, & De Marco, 2008; Werling & Debenedetti, 1999).

In this work, the simultaneous SAS fractionation and precipitation of a licorice ethanolic extract to produce micro- and nano-particles was studied for the first time. The effect of process parameters on the recovery of licorice antioxidants was analyzed, along with the morphology and particle size distribution of the precipitates.

2. Materials and methods

2.1 Chemicals

CO_2 (99.98 % purity) was supplied from Carburos Metálicos (Madrid, Spain). Ethanol (99.8 % purity), Sodium Carbonate anhydrous (99.5% purity) and Folin-Ciocalteu´s reagent were purchased from Panreac (Barcelona, Spain). Gallic acid standard (> 98% purity), 2,2-Diphenyl-1-pycrilhydrazyl (DPPH, 95% purity), (±)-6-Hydroxy-2,5,7,8-tetramethyllchromane-2-carboxylic acid (Trolox, 97% purity), liquiritin, liquiritigenin, isoliquiritigenin, glabridin and glycyrrhizic acid were purchased from Sigma–Aldrich (St. Louis, MO, USA). Orthophosphoric acid (85% purity) was purchased from Scharlab S.L. (Sentmenat, Spain). Acetonitrile (99,8% purity) was purchased from Macron (Poland).

2.2 Preparation of licorice ethanolic solutions

Roots of licorice harvested in Spain were obtained from Murciana herbalist's (Murcia, Spain) with water content of 9.90% wt. The sample was ground using a Grindomix GM 200 knife mill (Verder International B.V., Vleuten, Netherlands) in particles with size lower than 500 μm. Then, ultrasound assisted extraction (UAE) using an ultrasonic device (Branson Digital Sonifier 550 model, Danbury, USA) with an electric power of 550 W and frequency of 20 kHz was accomplished. The extraction was carried out at 323 K for 15 min using ethanol at 1:10 (w/v) plant/solvent ratio. Extraction yield was 3.18 % (mass of phytochemicals extracted / mass of plant material utilized) and the concentration of licorice phytochemicals in the ethanolic solution was 14.2 mg/ml (LES1). This ethanolic solution (704.2 ml) was further diluted with ethanol to a final volume of 1000 ml to obtain another ethanolic solution containing 9.6 mg/ml (LES2) of licorice phytochemicals. Both ethanolic solutions (14.2 mg/mL and 9.6 mg/mL) were stored at 253.15 K for its use in the SAS process.

2.3 Supercritical antisolvent (SAS) precipitation

Figure 1 shows the supercritical antisolvent precipitation device used for this study (Model Thar SF2000, Thar Technology, PA, USA). A detailed description of the equipment can be found elsewhere [36]. The equipment comprises a precipitation vessel and a separator with independent control of temperature and pressure. The precipitation vessel (273 ml) is equipped with a 101.6 μm inner diameter nozzle to spray the ethanolic solution. $SCCO_2$ and the ethanolic solution are fed from the top in a co-current manner (coaxial nozzle).

$SCCO_2$ was pumped at 50 g/min flow rate until pressure and temperature conditions were attained into the precipitation vessel. Then, the licorice ethanolic solution (LES) was pumped through the nozzle at 2 g/min for 45 min, while maintaining the $SCCO_2$ flow rate. Additional $SCCO_2$ was pumped during 15 min to wash out the residual solvent from the precipitator. During the process, the separator was kept at 313.15 K and ambient pressure. In the separator, ethanol and the phytochemicals which did not precipitate into the precipitation vessel (i.e. the licorice phytochemicals which are soluble in the $SCCO_2$+ethanol supercritical phase) were recovered. Finally, the

precipitation vessel was depressurized, and the precipitate was collected from a frit placed at the bottom of the precipitator vessel. The ethanolic fraction was further rotary evaporated until an oleoresin-type product was obtained. Samples (oleoresins and precipitates) were kept at 253.15 K under darkness until analysis.

2.4 Total phenolic compounds and antioxidant activity

Folin-Ciocalteu method (Singleton, Orthofer, & Lamuela-Raventós, 1999) was used to determine the total phenolic compounds (TPC) content in the samples. In order to determine the antioxidant capacity of the samples RPPH assa y was done following the procedure describe by Brand-Williams, Cuvelier, & Berset, (1995). All analyses were done in triplicate.

2.5 HPLC-DAD analysis

HPLC analysis was carried out as described by Wei, Yang, Chen, Wang, & Cui, (2015). A LC-2030C 3D Plus (Shimadzu) device equipped with a quaternary pump, auto-injector and DAD detector was used. The column was ACE Kromasil 100 C18 (250 x 4.6 mm; 5 μm) and analyses were accomplished at 298 K. The mobile phase comprised acetonitrile (A) and 0.026% aqueous H_3PO_4 (v/v), and the following elution gradient was applied: 20-25% A for 0-20 min, 25-34% A for 20-30 min, 34-50% A for 30-50 min, 50-60% A at 50-60 min and 60% A for 60-80 min. The initial conditions were attained in 5 min. The flow rate was 0.7 ml/min and was kept constant throughout the analysis. The injection volume was 20 μl and the detections were carried out at 230, 254, 280 and 370 nm. Calibration curves with standards were used to determine the content of the bioactive licorice phytochemicals (liquiritin, liquiritigenin, isoliquiritigenin, glabridin and glycyrrhizic acid) in the different samples.

2.6 Morphology and Particle size analysis

The morphology of precipitates was studied by scanning electron microscopy (SEM) with an energy-dispersive X-ray spectrometer (SEM-EDS) XL-30S FEG, Philips (Japan). Samples were placed on carbon tapes and then were coated with a thin chrome layer by a sputter coater. Particle size and size distributions were measured by light

147 scattering with a laser diffraction system Mastersizer 2000 (Malvern Instruments Ltd.,
148 Malvern, UK), equipped with a wet dispersion unit.

149 **3. Results and Discussion**

150 **3.1 The supercritical antisolvent process**

151 The CO_2 + ethanol + licorice phytochemicals is a complex multicomponent system and
152 the phase equilibria of this mixture strongly affect the performance and the result of
153 SAS process. The temperature and pressure of the mixture critical point (MCP) in
154 comparison with SAS temperature and pressure conditions may determine the success
155 of the precipitation process, since affect jet mixing, fluid dynamics and mass transfer
156 (Reverchon et al., 2010). These complex mechanisms are responsible for the great
157 variety of particle sizes and morphologies that can be obtained in SAS precipitation
158 process; it was described in the literature (Reverchon et al., 2010), these mechanisms
159 strongly depend on the SAS temperature and pressure conditions, which can be located
160 below the MCP, near above the MCP or far above the MCP Figure 2).

161 In general, it was stated (Reverchon & De Marco, 2011) that when SAS conditions are
162 below the MCP but in the homogenous subcritical region, the formation of particles is
163 induced by the $SCCO_2$ antisolvent effect and by the organic solvent depletion in the
164 droplets formed by the nozzle. Consequently, microparticles and expanded
165 microparticles (hollow core particles) with irregular forms are obtained. Nevertheless, if
166 the SAS subcritical conditions are located within the liquid-vapor region, irregular
167 particles and agglomerates are produced due to the presence of residual solvent in the
168 precipitate. On the other hand, when SAS conditions are far above the MCP, the mixing
169 of CO_2 with the solvent is produced instantaneously and no liquid-gas interphase
170 occurs, resulting in smaller and more regular particles due to their condensation from a
171 gaseous phase.

172 Due to the lack of information about phase equilibria of the complex mixtures CO_2 +
173 ethanol + licorice phytochemicals, the $SCCO_2$ and licorice ethanolic solution (LES)
174 flow rates were established with the aim of attaining a homogenous supercritical phase
175 (≈ 3 % mass ethanol) at the pressures and temperatures studied, according to the CO_2 +

ethanol binary phase equilibria data (C. J. Chang, Day, Ko, & Chiu, 1997; Joung et al., 2001; Knez, Škerget, Ilič, & Lütge, 2008; Reverchon & De Marco, 2011). Indeed, this is an approximation, since the presence of a large number and varied phytochemicals in the supercritical phase may really change the MPC in comparison with that of the binary CO_2 + ethanol.

3.2. Effect of the concentration of phytochemicals in the licorice ethanolic solution

Table 1 shows the results obtained by SAS with LES1 (14.2 mg/ml) at different precipitation pressures and temperatures, reporting the precipitate and oleoresin yields, TPC, TEAC and IC_{50} values. All SAS experiments were carried out by duplicate and the average deviations are given (Table 1).

A significant decrease in the precipitation yields was observed at 313.15 K (experiments 1 and 2 in Table 1) in comparison with the rest of experiments. These precipitates were very viscous, with large agglomerates adhered to the precipitation vessel walls, and they were difficult to recover and to quantify their weight and thus, high deviations were obtained. On the other hand, for the rest of experiments reported in Table 1, which were performed at 308.15 K, solid and dry powders were obtained, and the average deviation of precipitation yields between duplicates was always less than 9.21 % (mean deviation of 3.96 %).

Table 2 show SAS precipitation assays when the concentration of the licorice ethanolic solution was 9.6 mg/ml (LES2). Experiments were carried out at 308.15 and 313.15 K and pressures of 15 and 20 MPa. No duplicates were accomplished and thus, no average deviations are given for process yields. Yet, the TPC, antioxidant activity (TEAC and IC_{50} values) determinations were carried out by triplicate and the average deviations of these data are included in Table 2.

In all the experiments reported in Table 2, homogeneous particles were obtained in dry powders, including those assays carried out at 313.15 K. The different behavior observed at this temperature when using the different licorice ethanolic solutions, may be due to an expected higher MCP of LES1 in comparison with the MCP of LES2, as a result of the higher concentration of phytochemicals in LES1. Thus, it is possible that

SAS operation conditions were subcritical for LES1 while supercritical for LES2. Furthermore, higher concentration of phytochemicals results in higher solution viscosity and may impair atomization, as reported by Prosapio, De Marco, & Reverchon, (2018). Then, experiments with LES1 at 313.15 K lead to the coalescence of particles, forming agglomerates, while experiments with LES2 at the same temperature resulted in dry powders.

Additionally, it can be observed from Tables 1 and 2 that precipitate, and oleoresin yields were higher using LES2 than using LES1. Thus, the total yields of SAS process (precipitate + oleoresin) were higher at the lower concentration of the licorice ethanolic solution used. For example, experiment 7 in Table 2 shows a 1.5-fold increase of process yield (91 %) in comparison with its counterpart at 14.2 mg/ml (experiment 4 in Table 1).

3.2. Effect of pressure and temperature in SAS process yields

Figure 3 shows that at constant temperature (308.15 K) and constant licorice ethanolic concentration (LES1) the lower pressures brought about higher precipitate yields than oleoresin yields, while the opposite effect occurred at the higher pressures. As the pressure in the precipitation vessel increases at constant temperature, the $SCCO_2$ density increases and thus, the solubility of licorice phytochemicals in the supercritical phase also increases, resulting in a decrease of precipitation yield. Then, while lower amounts of solid powders are recovered in the precipitates, larger amounts of oleoresins are recovered from the separator. Furthermore, it can be observed that total recovery (mass of precipitate + oleoresin) of licorice phytochemicals feed into the SAS process reached values in the range 58-67% (experiments 3-6 in Table 1).

The general tendency observed with LES1 concerning the effect of pressure was also observed with LES2 (i.e. exp. 7 and 8 at 308.15 K, and exp. 9 and 10 at 313.15 K) but the total recovery of licorice phytochemicals in this case was higher and in the range of 68-91% (Table 2).

Regarding the effect of temperature, it can be observed that at lower pressures a decrease in temperature favors the precipitate yields, as indicated by the results of Table

1 (exp. 1 and 4) and Table 2 (exp. 7 and 9), all them carried out at 15 MPa. Consequently, the increase in temperature produced an increase in the oleoresin yields. However, at the higher pressures (20 MPa) the effect of temperature seems to be less important.

3.2 Phenolic compounds and antioxidant activity of precipitates and oleoresins

Figure 4 shows the recovery of total phenolic compounds obtained in the precipitation vessel as a function of pressure and concentration of licorice phytochemicals in the ethanolic solution. The TPC recoveries were higher with the lower concentration of the licorice ethanolic solution. Furthermore, a tendency to obtain higher TPC recoveries at the lower pressures can also be observed. Within the range of SAS operation conditions studied, the best conditions to recover in the precipitate the licorice phenolic compounds would be 15 MPa, 308.15 K and 9.6 mg/ml licorice ethanolic solution. At these conditions high concentration (160.8 mg GAE/g) and yield (≈ 71 %) of TPC was obtained, and also adequate precipitation yield (52.7%) was achieved. Taking into account that the original licorice root ultrasound extract contains 119.5 ± 4.1 mg GAE/g, an increase in the concentration of TPC was observed in the precipitates, with values up to 1.4 greater.

Since phenolic compounds are substances with recognized antioxidant activity it is generally stated that the higher the TPC the higher the antioxidant activity, that is the higher TEAC values and the lower IC_{50} values. The TEAC and IC_{50} values obtained in precipitates and oleoresins are depicted in Figure 5 as a function of TPC. In general, as can be observed in Figure 5(a), there is no clear relationship (e.g. linear relation) between TEAC and TPC values but is apparent that the precipitates presented higher TEAC values than oleoresins for the same TPC concentration. This means that different type and phenolic compound composition are present in precipitates and oleoresins, being the TPC in the precipitate of greater antioxidant capacity. Accordingly, the IC_{50} values of the precipitates are lower than those corresponding to oleoresins, as can be seen in Figure 5(b).

3.3 SAS fractionation of licorice phytochemicals

As mentioned before, in the case of SAS precipitation of ethanolic plant extracts, the fractionation of its bioactive substances is generally carried out, due to the different solubility of the plant extract components in the supercritical CO_2 + ethanol phase (Villanueva-Bermejo et al., 2017; Villanueva Bermejo et al., 2015).

Table 3 presents some key licorice bioactive compounds (Figure 6) identified in both, precipitates and oleoresins. In general, liquiritigenin, glabridin and isoliquiritigenin compounds are more abundant in the oleoresins, while liquiritin and glycyrrhizic acid are concentrated in the precipitates. The observed trend may be explained considering the polarity of these compounds, which is related to their chemical structure.

The most polar compounds are less soluble in the supercritical phase (CO_2 + ethanol cosolvent) and thus these polar compounds should preferable precipitate. On the contrary, the less polar compounds (more soluble in the supercritical phase) should be preferable recovered in the separator, together with the ethanol cosolvent. Both liquiritigenin and glabridin are the most non-polar compounds identified, with only two hydroxyl groups in their structure. Isoliquiritigenin has a structure similar to liquiritigenin but the latter is a flavanone and isoliquiritigenin is a chalcone (flavanone precursor). The chalcones have the central ring open, so they have a free hydroxyl group that gives it greater polarity compared to the flavone liquiritigenin. Glycyrrhizic acid is a glycosylated terpenoid, and despite its terpenoid part, the glycosylated sugar provides some polarity to this acid, producing its concentration in the precipitate. Finally, liquiritin is the most polar compound of those studied (with 5 hydroxyl groups in its chemical structure) and it is observed that it is most abundant in the precipitate.

Figure 7 shows for experiments 3 to 6 (308.15 K and 14.2 mg/ml of the licorice ethanolic solution) the variation with pressure of the precipitate IC_{50} values and the sum of the concentrations (mg/g) of the compounds identified and quantified by HPLC (Table 3). The IC_{50} values decrease with decreasing pressure while the content of these compounds in the precipitates increases. That is, the precipitates present better antioxidant activity and contain large amounts of licorice key bioactives at the lower precipitation pressures. This trend was verified for the sum of the concentrations of all identified compounds, as well as for the concentration of liquiritin and glabridin, which

293 are the most abundant compounds within those identified. Therefore, it could be
294 concluded that key licorice root compounds of Table 3 have a significant effect on the
295 antioxidant activity of the precipitates. This conclusion is in accordance with Kaur et al.,
296 (2013), who pointed out glabridin and isoliquiritigenin as key compounds responsible
297 for the antioxidant activity of licorice root.

298 **3.4 Morphology and particle size of precipitates**

299 Taking into account the phase equilibria of the binary CO_2 + ethanol mixture [43-45]
300 the corresponding critical pressures at 308.15 K and 313.15 K are both lower than 10
301 MPa. Thus, considering the binary mixture, the operating conditions set for all the
302 experiments in Tables 1 and 2 should be above the MCP (supercritical homogeneous
303 phase region of Figure 2) and no liquid-gas interphase should occur, which could lead to
304 the formation of small and uniform particles. Nevertheless, as stated before, in the case
305 of the precipitation of vegetal extracts, the presence of a large variety of phytochemicals
306 in the organic solution may change significantly the MCP of the supercritical phase.
307 Figure 8 shows the morphology (SEM imagens) resulted in experiments 1 and 2 of
308 Table 1. As can be clearly deduced from the figure, the morphology obtained in
309 experiments 1 and 2 are very different from those resulted in the rest of experiments. A
310 semi-continuous material is observed, more similar to a gum-resin, with cavities within
311 the aggregates. These images might corroborate that SAS operating conditions in these
312 experiments were below the MCP, probably in the two-phase region of Figure 2, as a
313 result of the higher temperature and higher concentration of phytochemicals in the
314 ethanolic solution. Figure 9 show SEM imagens at a lower scale (75x) of the
315 precipitates obtained in experiments 1 and 2, where it can be observed adjoined particles
316 (coalescence phenomenon) in large sizes, especially at 15 MPa (experiment 1).

317 On the other hand, for the rest of experiments of Figure 8, particles with similar
318 morphology and micronized size were obtained. Nevertheless, uniform and spherical
319 structures in the precipitates were not obtained probably due to precipitation conditions
320 in the subcritical region (see Figure 2) since, as mentioned before, uniform and small
321 spherical particles (nanoparticles) are generally obtained at pressures larger than those

corresponding to the MCP (Reverchon et al., 2008, 2010; Werling & Debenedetti, 2000).

The mean particle size and size distribution of the precipitates are given in Table 4. Furthermore, for experiments 3 to 6 the particle size distributions of duplicate experiments are depicted in Figure 10. Deviations are in the range 1.1-3.4 μm (< 10%). It can be observed that at constant temperature (308.15 K) and concentration of the licorice ethanolic solution (14.2 mg/g) the mean particle size of the precipitated powders decreases with pressure, from 36.7 μm at 12.5 MPa to 11.7 μm at 25 MPa. In addition, it could be inferred from Figure 10 that at the higher pressures the particle sizes are somewhat more heterogeneous. The distribution at the lower pressure (12.5 MPa) is narrower and more normal, while increasing pressure the behavior appears as a multi-modal distribution, with significant smaller sizes.

This tendency of particle size decrease with an increase in the precipitation pressure is consistent with the analysis published by Werling & Debenedetti, (1999) and Martín & Cocero, (2004) in their SAS precipitation simulation models. Furthermore, several experimental works confirm this tendency, such as the SAS precipitation of tartaric acid reported by Kröber & Teipel, (2002), the *Achilea millefolium* L. ethanolic extract studied by Villanueva-Bermejo et al., (2017), and mango leaf extracts carried out by Guamán-Balcázar et al., (2019).

Besides the effect of pressure on particle size, it can be observed in the SEM imagens presented in Figure 11 that decreasing the concentration of the licorice ethanolic solution smaller particles are obtained. The lower the concentration of licorice phytochemicals in the ethanolic solution, the more similar MCP of the supercritical phase to that of the binary CO_2 + ethanol, and thus the precipitation conditions established are closer to be in the supercritical homogenous region.

4. Conclusions

Selecting adequate operating conditions, the supercritical anti-solvent SAS precipitation of licorice ethanolic solutions produced the fractionation of licorice phytochemicals: dry powders with small aggregate particles together with oleoresin by-product were

obtained. The higher precipitation yields were obtained at the lower pressures and temperatures, and yield increases as the concentration of licorice phytochemicals in the ethanolic solution decreases from 14.2 to 9.6 mg/ml, being the highest yield (52.70%) obtained at 15MPa, 308.15 K and 9.6 mg/ml.

In general, it was observed an increase of the recovery of phenolic phytochemicals in the precipitates as the pressure, temperature and concentration of the licorice ethanolic solution decreases. Within the operating range studied, the optimum corresponds to 15 MPa, 308.15 K and 9.6 mg/ml, with a 1.3 enrichment factor with respect to the licorice extract. Furthermore, the precipitates have better antioxidant activity than the oleoresins for the same concentration of total phenolic compounds, due to the fractionation caused by SAS technique resulting in different type of phenolic compounds in precipitates and oleoresins. Liquiritin and glabridin are abundant in the precipitates, and the IC_{50} values decrease (better antioxidant activity) as their concentration in the precipitates increases.

Particles with smaller size were obtained with increasing pressure and decreasing the concentration of phytochemicals in the licorice ethanolic solution. Nevertheless, agglomerated particles were obtained, probably due to precipitation conditions in the range below the supercritical multicomponent (phytochemicals + CO_2 + ethanol) mixture critical point. It is highlighted the importance of SAS operating conditions well above the critical point of the supercritical mixture to obtain an adequate morphology with regular and spherical particles.

Acknowledgement

The authors gratefully acknowledge the financial support from Ministerio de Economía y Competitividad of Spain (Projects AGL2017-89055-R and AGL2016-76736-C3-1-R). Somaris E. Quintana is grateful for the funding provided by Gobernación de Bolivar and Fundación Ceiba, Colombia, in the project “Bolívar Gana con Ciencia”.

References

Baek, J. Y., Lee, J. M., & Lee, S. C. (2008). Extraction of nutraceutical compounds from licorice roots with subcritical water. *Separation and Purification Technology*, *63*(3), 661–664. https://doi.org/10.1016/j.seppur.2008.07.005

Brand-Williams, W., Cuvelier, M. E., & Berset, C. (1995). Use of a Free Radical Method to Evaluate Antioxidant Activity, *28*, 25–30.

Chang, C. J., Day, C. Y., Ko, C. M., & Chiu, K. L. (1997). Densities and P-x-y diagrams for carbon dioxide dissolution in methanol, ethanol, and acetone mixtures. *Fluid Phase Equilibria*, *131*(1–2), 243–258. https://doi.org/10.1016/s0378-3812(96)03208-6

Chang, X., Bao, J., Shan, G., Bao, Y., & Pan, P. (2017). Crystallization-Driven Formation of Diversified Assemblies for Supramolecular Poly(lactic acid)s in Solution. *Crystal Growth & Design*, *17*(5), 2498–2506. https://doi.org/10.1021/acs.cgd.7b00013

Chin, Y.-W., Jung, H.-A., Liu, Y., Su, B.-N., Castoro, J. A., Keller, W. J., … Kinghorn, A. D. (2007). Anti-oxidant Constituents of the Roots and Stolons of Licorice (Glycyrrhiza glabra). https://doi.org/10.1021/jf0703553

De Marco, I., Knauer, O., Cice, F., Braeuer, A., & Reverchon, E. (2012). Interactions of phase equilibria, jet fluid dynamics and mass transfer during supercritical antisolvent micronization: The influence of solvents. *Chemical Engineering Journal*, *203*, 71–80. https://doi.org/10.1016/J.CEJ.2012.06.129

Guamán-Balcázar, M. C., Montes, A., Pereyra, C., & Martínez de la Ossa, E. (2019). Production of submicron particles of the antioxidants of mango leaves/PVP by supercritical antisolvent extraction process. *Journal of Supercritical Fluids*, *143*(July 2018), 294–304. https://doi.org/10.1016/j.supflu.2018.09.007

Hedayati, A., & Ghoreishi, S. M. (2015). Supercritical carbon dioxide extraction of glycyrrhizic acid from licorice plant root using binary entrainer: Experimental optimization via response surface methodology. *Journal of Supercritical Fluids*, *100*, 209–217. https://doi.org/10.1016/j.supflu.2015.03.005

Joung, S. N., Yoo, C. W., Shin, H. Y., Kim, S. Y., Yoo, K. P., Lee, C. S., & Huh, W. S.

406 (2001). Measurements and correlation of high-pressure VLE of binary CO 2 -
407 alcohol systems (methanol, ethanol, 2-methoxyethanol and 2-ethoxyethanol). *Fluid*
408 *Phase Equilibria*, *185*(1–2), 219–230. https://doi.org/10.1016/S0378-
409 3812(01)00472-1

410 Kaur, R., Kaur, H., & Dhindsa, A. S. (2013). Glycyrrhiza glabra: a
411 phytopharmacological review. *International Journal of Pharmaceutical Sciences*
412 *and Research*, *4*(7), 2470–2477. https://doi.org/10.13040/IJPSR.0975-
413 8232.4(7).2470-77

414 Knez, Ž., Škerget, M., Ilič, L., & Lütge, C. (2008). Vapor-liquid equilibrium of binary
415 CO2-organic solvent systems (ethanol, tetrahydrofuran, ortho-xylene, meta-xylene,
416 para-xylene). *Journal of Supercritical Fluids*, *43*(3), 383–389.
417 https://doi.org/10.1016/j.supflu.2007.07.020

418 Kröber, H., & Teipel, U. (2002). Materials processing with supercritical antisolvent
419 precipitation: Process parameters and morphology of tartaric acid. *Journal of*
420 *Supercritical Fluids*, *22*(3), 229–235. https://doi.org/10.1016/S0896-
421 8446(01)00124-3

422 Langa, E., Pardo, J. I., Giménez-Rota, C., González-Coloma, A., Hernáiz, M. J., &
423 Mainar, A. M. (2019). Supercritical anti-solvent fractionation of Artemisia
424 absinthium L. conventional extracts: tracking artemetin and casticin. *Journal of*
425 *Supercritical Fluids*, *151*, 15–23. https://doi.org/10.1016/j.supflu.2019.05.003

426 Lee, H.-J., Kang, J.-H., Lee, H.-G., Kim, D.-W., Rhee, Y.-S., Kim, J.-Y., … Park, C.-
427 W. (2016). Preparation and physicochemical characterization of spray-dried and
428 jet-milled microparticles containing bosentan hydrate for dry powder inhalation
429 aerosols. *Drug Design, Development and Therapy*, *Volume 10*, 4017–4030.
430 https://doi.org/10.2147/DDDT.S120356

431 Martín, A., & Cocero, M. J. (2004). Numerical modeling of jet hydrodynamics, mass
432 transfer, and crystallization kinetics in the supercritical antisolvent (SAS) process.
433 *Journal of Supercritical Fluids*, *32*(1–3), 203–219.
434 https://doi.org/10.1016/j.supflu.2004.02.009

435 Martín, A., & Cocero, M. J. (2008). Micronization processes with supercritical fluids:
436 Fundamentals and mechanisms. *Advanced Drug Delivery Reviews*, *60*(3), 339–

350. https://doi.org/10.1016/J.ADDR.2007.06.019

Morita, T., Horikiri, Y., Suzuki, T., & Yoshino, H. (2001). Preparation of gelatin microparticles by co-lyophilization with poly(ethylene glycol): Characterization and application to entrapment into biodegradable microspheres. *International Journal of Pharmaceutics*, *219*(1–2), 127–137. https://doi.org/10.1016/S0378-5173(01)00642-1

Pan, X., Liu, H., Jia, G., & Shu, Y. Y. (2000). Microwave-assisted extraction of glycyrrhizic acid from licorice root. *Biochemical Engineering Journal*, *5*(3), 173–177. https://doi.org/10.1016/S1369-703X(00)00057-7

Prosapio, V., De Marco, I., & Reverchon, E. (2018). Supercritical antisolvent coprecipitation mechanisms. *The Journal of Supercritical Fluids*, *138*, 247–258. https://doi.org/10.1016/J.SUPFLU.2018.04.021

Quintana, S. E., Cueva, C., Villanueva-Bermejo, D., Moreno-Arribas, M. V., Fornari, T., & García-Risco, M. R. (2019). Antioxidant and antimicrobial assessment of licorice supercritical extracts. *Industrial Crops and Products*, *139*. https://doi.org/10.1016/j.indcrop.2019.111496

Rasenack, N., & Müller, B. W. (2004). Micron-Size Drug Particles: Common and Novel Micronization Techniques. *Pharmaceutical Development and Technology*. https://doi.org/10.1081/PDT-120027417

Reverchon, E., Adami, R., Caputo, G., & De Marco, I. (2008). Spherical microparticles production by supercritical antisolvent precipitation: Interpretation of results. *The Journal of Supercritical Fluids*, *47*(1), 70–84. https://doi.org/10.1016/J.SUPFLU.2008.06.002

Reverchon, E., & De Marco, I. (2011). Mechanisms controlling supercritical antisolvent precipitate morphology. *Chemical Engineering Journal*, *169*(1–3), 358–370. https://doi.org/10.1016/J.CEJ.2011.02.064

Reverchon, E., Torino, E., Dowy, S., Braeuer, A., & Leipertz, A. (2010). Interactions of phase equilibria, jet fluid dynamics and mass transfer during supercritical antisolvent micronization. *Chemical Engineering Journal*, *156*(2), 446–458. https://doi.org/10.1016/j.cej.2009.10.052

Sankeshwari, R., Ankola, A., Bhat, K., & Hullatti, K. (2018). Soxhlet versus cold maceration: Which method gives better antimicrobial activity to licorice extract against Streptococcus mutans? *Journal of the Scientific Society*, *45*(2), 67. https://doi.org/10.4103/jss.jss_27_18

Saxena, S. (2005). Natural Product Radiance Glycyrrhiza glabra: Medicine over the millennium. *Natural Product Radiance*, *4*(5), 358–367.

Singleton, V. L., Orthofer, R., & Lamuela-Raventós, R. M. (1999). [14] Analysis of total phenols and other oxidation substrates and antioxidants by means of folin-ciocalteu reagent. *Methods in Enzymology*, *299*, 152–178. https://doi.org/10.1016/S0076-6879(99)99017-1

Villanueva-Bermejo, D., Zahran, F., Troconis, D., Villalva, M., Reglero, G., & Fornari, T. (2017). Selective precipitation of phenolic compounds from Achillea millefolium L. extracts by supercritical anti-solvent technique. *Journal of Supercritical Fluids*, *120*, 52–58. https://doi.org/10.1016/j.supflu.2016.10.011

Villanueva Bermejo, D., Ibáñez, E., Reglero, G., Turner, C., Fornari, T., & Rodriguez-Meizoso, I. (2015). High catechins/low caffeine powder from green tea leaves by pressurized liquid extraction and supercritical antisolvent precipitation. *Separation and Purification Technology*, *148*, 49–56. https://doi.org/10.1016/j.seppur.2015.04.037

Visentin, A., Rodríguez-Rojo, S., Navarrete, A., Maestri, D., & Cocero, M. J. (2012). Precipitation and encapsulation of rosemary antioxidants by supercritical antisolvent process. *Journal of Food Engineering*, *109*, 9–15. https://doi.org/10.1016/j.jfoodeng.2011.10.015

Wang, W., Liu, G., Wu, J., & Jiang, Y. (2013). Co-precipitation of 10-hydroxycamptothecin and poly (l-lactic acid) by supercritical CO2 anti-solvent process using dichloromethane/ethanol co-solvent. *Journal of Supercritical Fluids*, *74*, 137–144. https://doi.org/10.1016/j.supflu.2012.11.022

Wei, S.-S., Yang, M., Chen, X., Wang, Q.-R., & Cui, Y.-J. (2015). Simultaneous determination and assignment of 13 major flavonoids and glycyrrhizic acid in licorices by HPLC-DAD and Orbirap mass spectrometry analyses. *Chinese Journal of Natural Medicines*, *13*(3), 232–240. https://doi.org/10.1016/S1875-

5364(15)30009-1

Werling, J. O., & Debenedetti, P. G. (1999). Numerical modeling of mass transfer in the supercritical antisolvent process. *The Journal of Supercritical Fluids*, *16*(2), 167–181. https://doi.org/10.1016/S0896-8446(99)00027-3

Werling, J. O., & Debenedetti, P. G. (2000). Numerical modeling of mass transfer in the supercritical antisolvent process: Miscible conditions. *Journal of Supercritical Fluids*, *18*(1), 11–24. https://doi.org/10.1016/S0896-8446(00)00054-1